Hindawi
Advances in Astronomy
Volume 2023, Article ID 9434141, 18 pages
https://doi.org/10.1155/2023/9434141

Research Article

Restricted Concave Kite Five-Body Problem

A. R. Kashif [1] **and M. Shoaib** [2]

[1]*Department of Mathematics, Capital University of Science and Technology, Zone-V, Islamabad, Pakistan*
[2]*Smart and Scientific Solutions, 32 Allerdyce Drive, Glasgow G156RY, UK*

Correspondence should be addressed to A. R. Kashif; kashmology@gmail.com

Received 1 February 2022; Revised 30 November 2022; Accepted 19 January 2023; Published 19 April 2023

Academic Editor: Kovacs Tamas

The restricted concave kite five-body problem is a problem in which four positive masses, called the primaries, rotate in the concave kite configuration with a mass at the center of the triangle formed by three of the primaries. The fifth body has negligible mass and does not influence the motion of the four primaries. It is assumed that the fifth mass is in the same plane of the primaries and that the masses of the primaries are m_1, m_2, m_3, and m_4, respectively. Three different types of concave kite configurations are considered based on the masses of the primaries. In case I, one pair of primaries has equal masses; in case II, two pairs of primaries have equal masses; in case III, three of the primaries have equal masses. For all three cases, the regions of central configuration are obtained using both analytical and numerical techniques. The existence and uniqueness of equilibrium positions of the infinitesimal mass are investigated in the gravitational field of the four primaries. It is numerically confirmed that none of the equilibrium points are linearly stable. The Jacobian constant C is used to investigate the regions of possible motion of the infinitesimal mass.

1. Introduction

Dynamical systems with few bodies (three) have been extensively studied in the past, and various models have been proposed for research aiming to approximate the behavior of real celestial systems. There are many reasons for studying the five-body problem besides the historical ones since it is known that approximately two-thirds of the stars in our Galaxy exist as part of multistellar systems. In this manuscript, the motion of a body of negligible mass under the Newtonian gravitational attraction of four bodies (called primaries) moving each one in circular periodic orbits around their center of mass is considered. At any instant of time, the primaries form a kite configuration (central configuration) which is a particular solution to the general five-body problem. Central configurations (CC) play a vital role in the understanding of the n-body problem of celestial mechanics. It can be used to find simple or special solutions to the n-body problem since the geometry formed by the arrangement of the primaries remains constant for all time (cf. Saari [1]; Moeckel [2]; Farantos [3]; Deng and Zhang [4]; MacMillan and Bartky [5]; Sim [6]; Llibre and Mello [7]; Papadakis and Kanavos [8]).

The restricted five-body problem mainly takes into consideration a fifth body generally referred to as the test particle with negligible mass and does not influence the motion of the four primaries. Kulesza et al. [9] discussed restricted rhomboidal five-body problem, and they found that 11, 13, or 15 equilibrium solutions are all unstable. Siddique et al. [10] did a stability analysis of the rhomboidal restricted six-body problem. Ansari and Alhussain [11] investigated the five-body problem with kite configuration where four bodies are placed at the vertices of a kite, and the fifth infinitesimal body is moving in the space under the influences of these four primaries but not influencing them gravitationally. After evaluating the equations of motion of the infinitesimal body, they investigated the location of Lagrange points and their linear stability, zero velocity curves, region of motion for the infinitesimal body, and Poincare surfaces of section. Shahbaz Ullah et al. [12] investigated the series solutions of the Sitnikov kite configuration by the methods given by Lindstedt-Poincaré, using

Green's function and MacMillan. Bengochea et al. [13] discussed the planar four-body problem emanating from a kite configuration with three equal masses by using analytical and numerical tools and showed the existence of families of quasiperiodic orbits. They introduced a new coordinate system that measures (in the planar four-body problem) how far an arbitrary configuration from a kite configuration is. Hampton [14] studied the finiteness of planar relative equilibria of the Newtonian five-body problem and the five-vortex problem in the case that configurations form a symmetric kite. They proved that the equivalence classes of such relative equilibria are finite with some possible exceptional cases. These exceptional cases are given explicitly as polynomials in the masses (or vorticities in the vortex problem). Álvarez-Ramírez and Llibre [15] using mutual distances as coordinates showed that any four-body central configuration forming a Hjelmslev quadrilateral must be a right kite configuration. A Hjelmslev quadrilateral is a quadrilateral with two right angles at opposite vertices.

In this work, we study the motion of a body of negligible mass under the Newtonian gravitational attraction of four bodies of masses $m_1, m_2, m_3,$ and m_4 (called primaries) moving each one in circular periodic orbits around their center of mass. At any instant of time, the primaries form a configuration (central configuration) of a concave kite which is a particular solution to the five-body problem. Here, we study the position of the infinitesimal mass, m_5, in the plane of motion of the primaries, and we use either the sideral system of coordinates or the synodic system of coordinates (see [4] or [8] for details). $r_1 = (-1, -\alpha), r_2 = (0, \beta), r_3 = (1, -\alpha), r_4 = (0, 0)$ where α and β are positive numbers. We call this as restricted concave kite five-body problem (RK5BP) (see Figure 1). The rest of the paper is organized as follows: in Section 2, we derive the general equations for (RK5BP) and list the main results. Three specific cases of CC's for four primaries are investigated. In Section 3, the equations of motion for m_5 are set up in synodic system of coordinates. We explore the hill region and possible region of motion of m_5 according to the Jacobian constant. In Section 4, we discuss, analytically, the equilibrium points along the coordinate axes and numerically off the axes for different cases of CCs. In Section 5, the linear stability of equilibrium points is discussed, and conclusions are drawn in the last section.

2. Four-Body Concave Kite Central Configurations

Érdi and Czirják [16] studied the planar central configurations of four bodies when two bodies are on an axis of symmetry, and the other two bodies have equal masses and are situated symmetrically with respect to the axis of symmetry and gave a complete solution for a symmetric case. The derived formulae represent exact analytical solutions of the four-body problem. They also discussed one convex and two concave cases of central configuration in detail. Benhammouda et al. [17] studied the central configuration of the kite four-body problems. They considered two different types of symmetrical configurations. In both cases, the existence of a continuous family of central

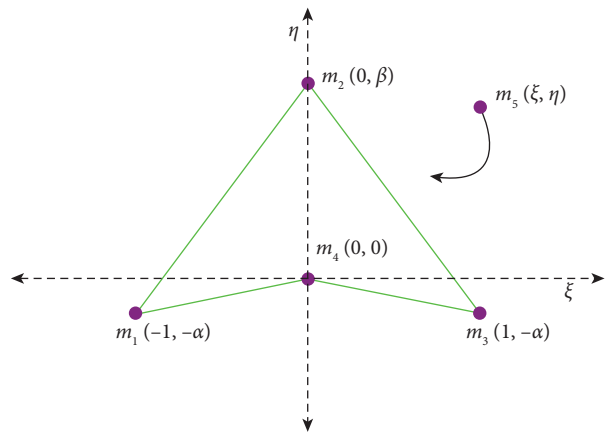

Figure 1: The restricted concave kite five-body problem.

configurations for positive masses is shown. They also provided numerical explorations via Poincaré cross sections, to show the existence of periodic and quasiperiodic solutions for the four-body problem. Hampton [18] discussed the existence of a new family of planar five-body central configurations. This family is unusual in that it is a stacked central configuration, i.e., a subset of the points also forms a central configuration. Mello and Fernandes [19] studied the existence of kite central configurations in the planar four-body problem which lies on a common circle. They also proved the existence of kite central configurations in the spatial five-body problem which lies on a common sphere. Perez-Chavela and Santoprete [20] proved that there is a unique convex noncollinear central configuration of the planar four-body problem when two equal masses are located at opposite vertices of a quadrilateral, and at most, only one of the remaining masses is larger than the equal masses. Such a central configuration possesses a symmetry line, and it is a kite-shaped quadrilateral. They also showed that there is exactly one convex noncollinear central configuration when the opposite masses are equal. Such a central configuration also possesses a symmetry line, and it is a rhombus. Corbera et al. [21] prove that any four-body convex central configuration with perpendicular diagonals must be a kite configuration. They extended the result to general power-law potential functions, including the planar four-vortex problem. Ansari et al. [22] presented a numerical investigation of some characteristics and parameters related to the motion of an infinitesimal body with variable mass in a five-body problem. The whole system forms a cyclic kite configuration. They also determined the positions of Lagrangian points and basins of attraction for the infinitesimal body. They also investigated the linear stability of the Lagrangian points and found that Lagrangian points are unstable.

We consider, initially, four primaries with masses $m_1 = m_3 = m$, m_2, and m_4 in a concave kite configuration. As it is a classical approach, in such cases, the system will be treated in a synodical system of coordinates in order to eliminate the time dependence. The whole system rotates with constant angular velocity, the centrifugal force compensates for the Newtonian attraction, and the five bodies are in equilibrium

in such a rotating system, the so-called "relative equilibria solutions." The central configuration of this particular was derived in [17], and we will give a brief review of their results with minor improvement.

If we denote by $\mathbf{r}_j$ the position of the body with mass m_j, and by $\mathbf{r}_{ij} = \|\mathbf{r}_j - \mathbf{r}_j\|$, the distance between the body with mass m_j and the body with mass m_i, then the algebraic system of equations that must be satisfied for the bodies to be in noncollinear central configuration is

$$f_{ij} = \sum_{k=0,k\neq i,j}^{n-1} m_k\left(R_{ik} - R_{jk}\right)\Delta_{ijk} = 0, \tag{1}$$

where $R_{ij} = r_{ij}^{-3}$ and $\Delta_{ijk} = |(\mathbf{r}_i - \mathbf{r}_j)\wedge(\mathbf{r}_i - \mathbf{r}_k)|$ represent the area of the triangle determined by the sides $\|\mathbf{r}_i - \mathbf{r}_j\|$ and $\|\mathbf{r}_i - \mathbf{r}_k\|$. After eliminating redundant equations due to the symmetries of the problem, i.e., $f_{13} = f_{24} \equiv 0$, $f_{12} = f_{23}$, $f_{14} = f_{34}$, and $m_1 = m_3$, [17], we get the following two equations:

$$\begin{aligned} f_{12} = {} & 2(\alpha+\beta)\left(\frac{1}{8} - \frac{1}{\left((\alpha+\beta)^2+1\right)^{(3/2)}}\right)m_1 \\ & + \beta\left(\frac{1}{\left(\alpha^2+1\right)^{(3/2)}} - \frac{1}{\beta^3}\right)m_4 = 0, \end{aligned} \tag{2}$$

$$\begin{aligned} f_{14} = {} & 2\alpha\left(\frac{1}{8} - \frac{1}{\left(\alpha^2+1\right)^{(3/2)}}\right)m_1 \\ & - \beta\left(\frac{1}{\left((\alpha+\beta)^2+1\right)^{(3/2)}} - \frac{1}{\beta^3}\right)m_2 = 0. \end{aligned} \tag{3}$$

We will consider three special cases based on the relationship between the masses:

Case I: $m_1 = m_3 = m \neq m_2 \neq m_4$

Case II: $m_1 = m_3$ and $m_2 = m_4$

Case III: $m_1 = m_2 = m_3 = m \neq m_4$

2.1. Case I: $m_1 = m_3 \neq m_2 \neq m_4$. Let

$$\begin{aligned} \mu_1 &= \frac{m_2}{m}, \\ \mu_2 &= \frac{m_4}{m}. \end{aligned} \tag{4}$$

Then, the simultaneous solution of equations (2) and (3) gives

$$\begin{aligned} \mu_1 &= \frac{\alpha\beta^2\left(\left(\alpha^2+1\right)^{(3/2)} - 8\right)\left((\alpha+\beta)^2+1\right)^{(3/2)}}{4\left(\alpha^2+1\right)^{(3/2)}\left(\beta^3 - \left((\alpha+\beta)^2+1\right)^{(3/2)}\right)}, \\ \mu_2 &= \frac{\beta^2(\alpha+\beta)\left(\alpha^2+1\right)^{(3/2)}\left(\left((\alpha+\beta)^2+1\right)^{(3/2)} - 8\right)}{4\left((\alpha+\beta)^2+1\right)^{(3/2)}\left(\left(\alpha^2+1\right)^{(3/2)} - \beta^3\right)}. \end{aligned} \tag{5}$$

With some elementary computations, the region of central configurations for positive masses is derived as follows:

$$\begin{aligned} R_{\mu_1\mu_2} = {} & \left(0 < \alpha < \frac{1}{\sqrt{3}} \wedge \sqrt{\alpha^2+1} < \beta < \sqrt{3} - \alpha\right) \\ & \vee\left(\alpha > \frac{1}{\sqrt{3}} \wedge \sqrt{3} - \alpha < \beta < \sqrt{\alpha^2+1}\right). \end{aligned} \tag{6}$$

The values of the mass ratios μ_1 and μ_2 are depicted in Figure 2.

2.2. Case II: $m_1 = m_3$ and $m_2 = m_4$. Let $m_1 = m_3 = \mu$ and $m_2 = m_4 = 1$, then equations (2) and (3) give

$$\begin{aligned} \mu &= \frac{4f_2\left(\beta^3 - f_1\right)}{\alpha\beta^2 f_1\left(f_2 - 8\right)}, \\ f(\alpha,\beta) &= \frac{1}{\beta^2} - \frac{\left(f_1 - 8\right)f_2(\alpha,\beta)\left(\beta^3 - f_1\right)}{\alpha\beta^2 f_1^2\left(f_2 - 8\right)} - \frac{\beta}{f_2}, \end{aligned} \tag{7}$$

where $f_1(\alpha,\beta) = (1 + (\alpha+\beta)^2)^{(3/2)}$ and $f_2(\alpha,\beta) = (1+\alpha^2)^{(3/2)}$. The function $f(\alpha,\beta) = 0$ is a necessary condition for the central configurations to exist. It is not possible to analytically solve $f(\alpha,\beta) = 0$ for either α or β, and therefore, we use interpolation to write $\beta = \varphi(\alpha)$, where

$$\begin{aligned} \varphi(\alpha) = {} & 2349.87\alpha^{12} - 16627.1\alpha^{11} + 52450.\alpha^{10} - 97275.4\alpha^9 \\ & + 117771.\alpha^8 - 97711.8\alpha^7 \\ & + 56737.3\alpha^6 - 23129.5\alpha^5 + 6542.32\alpha^4 - 1250.54\alpha^3 \\ & + 155.539\alpha^2 - 12.1183\alpha + 1.66263. \end{aligned} \tag{8}$$

This allows us to write $\mu := \mu(\alpha)$ which makes the quantitative analysis of μ significantly easier. The values of the mass ratio μ are depicted in Figure 3.

2.3. Case III: $m_1 = m_2 = m_3 \neq m_4$. Let $m_1 = m_2 = m_3 = 1$ and $\mu = m_4$, then equations (2) and (3) give

$$\begin{aligned} \mu(\alpha+\beta) &= \frac{\beta^2\left(f_1 - 8\right)f_2(\alpha+\beta)}{4f_1\left(f_2 - \beta^3\right)}, \\ f(\alpha,\beta) &= -\alpha\beta^2 f_1\left(f_2 - 8\right) + 4\beta^3 f_2 - 4f_1 f_2 = 0, \end{aligned} \tag{9}$$

where

$$\begin{aligned} f_1(\alpha,\beta) &= \left((\alpha+\beta)^2+1\right)^{(3/2)}, \\ f_2(\alpha+\beta) &= \left(\alpha^2+1\right)^{(3/2)}. \end{aligned} \tag{10}$$

The function $f(\alpha,\beta) = 0$ is a necessary condition for the central configurations to exist. It is not possible to analytically solve $f(\alpha,\beta) = 0$ for either α or β; therefore, we use interpolation to write $\beta = \phi(\alpha)$, where

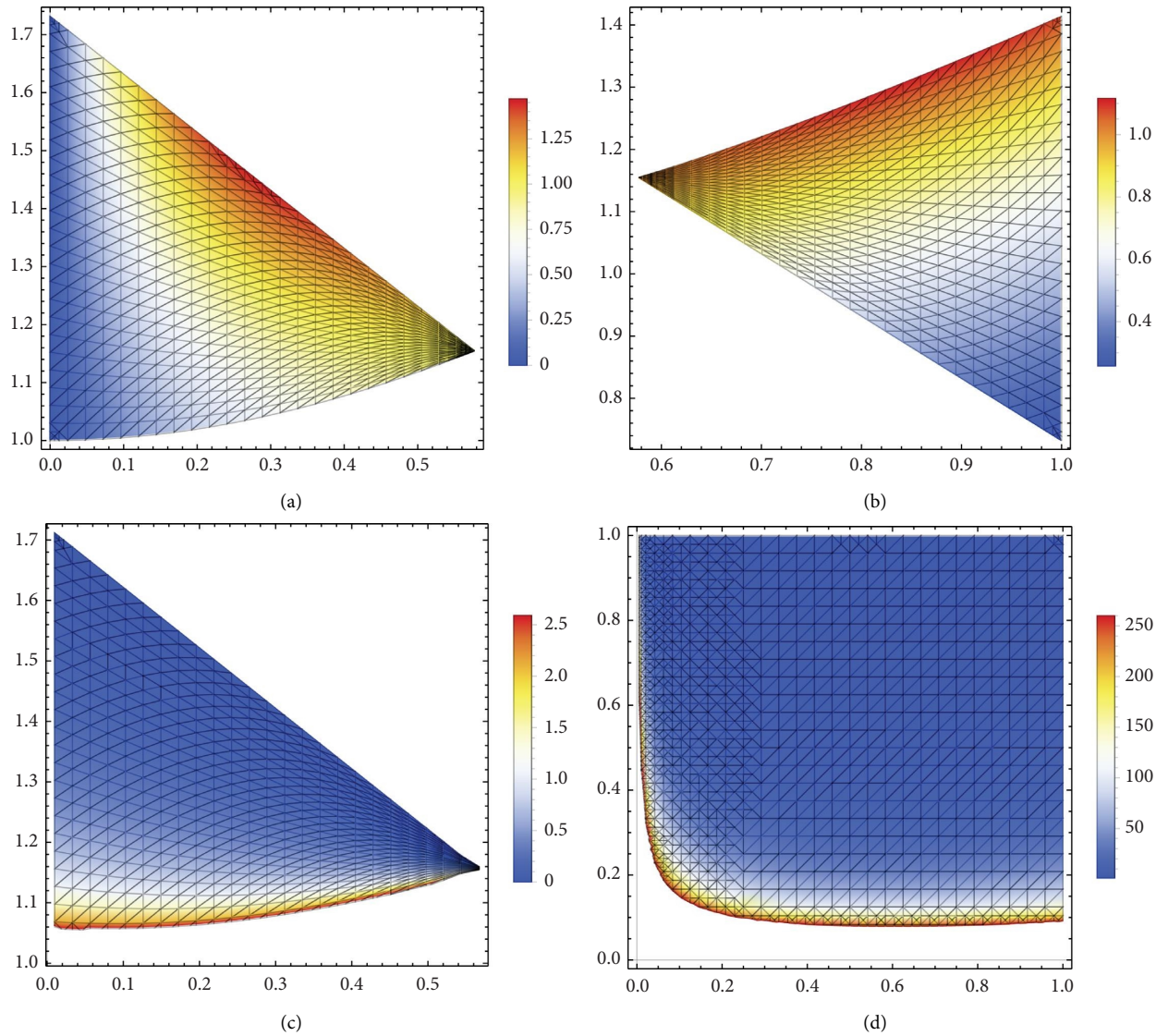

Figure 2: The mass ratios μ_1 and μ_2 in case I.

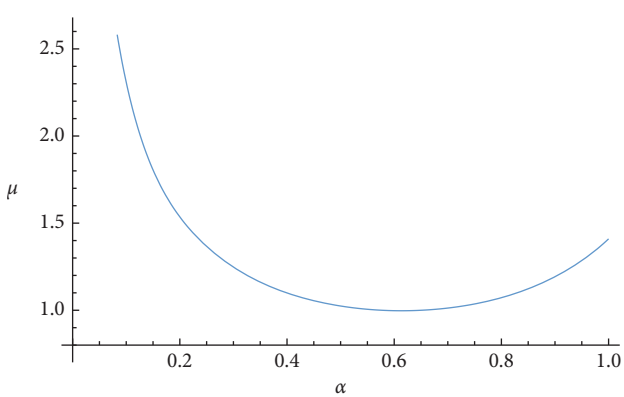

Figure 3: The mass ratios μ in case II.

$$\begin{aligned}\phi(\alpha) = {} & -46.7371\alpha^{11} + 366.213\alpha^{10} - 1282.56\alpha^{9} + 2650.35\alpha^{8} \\ & - 3592.55\alpha^{7} + 3358.82\alpha^{6} - 2217.15\alpha^{5} + 1040.41\alpha^{4} \\ & - 345.444\alpha^{3} + 80.8174\alpha^{2} - 13.2235\alpha + 2.40488 \\ & \text{and } \alpha \in (0.0994, 1).\end{aligned} \tag{11}$$

This allows us to write the mass ratio μ as a function of α only. The function $\mu(\alpha)$ is an increasing function and attains its maximum at $\alpha = 1$. The values of the mass ratios μ are depicted in Figure 4.

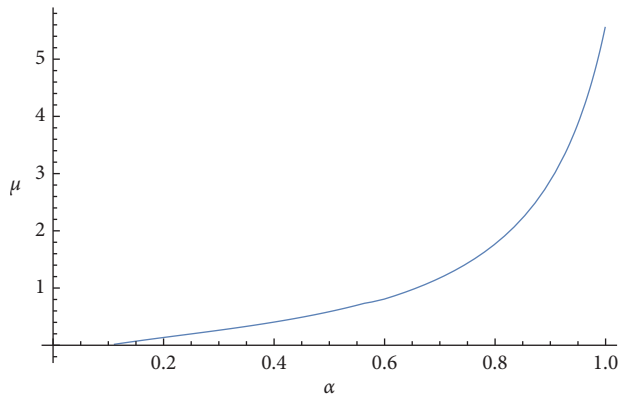

Figure 4: The mass ratios μ in case III.

3. Setting Up of the Problem and Preliminary Results

We consider the motion of an infinitesimal mass m_5 in the gravitational field of the concave kite configuration described in Section 2. The equations of motion of the body m_5 are

$$\begin{aligned} \ddot{\zeta} - 2\dot{\eta} &= \Omega_\zeta, \\ \ddot{\eta} + 2\dot{\zeta} &= \Omega_\eta, \end{aligned} \tag{12}$$

where

$$\begin{aligned} \Omega(\zeta,\eta) = {} & \frac{1}{2}\left(\zeta^2+\eta^2\right) \\ & + m\left(\frac{1}{\sqrt{(\eta+\alpha)^2+(\zeta+1)^2}} + \frac{1}{\sqrt{(\eta+\alpha)^2+(\zeta-1)^2}}\right) \\ & + \frac{m_2}{\sqrt{(\eta-\beta)^2+\zeta^2}} + \frac{m_4}{\sqrt{\zeta^2+\eta^2}}, \end{aligned} \tag{13}$$

is the effective potential.

Define a first Jacobi-type integral by

$$C = \frac{1}{2}\left(\dot{\zeta}^2+\dot{\eta}^2\right) - \Omega. \tag{14}$$

It is trivial to show that $C(\zeta,\eta)$ is the first integral of motion of the system (12) by proving that $\dot{C}(\zeta,\eta) = 0$.

3.1. The Hill Sphere and Region of Motion for m_5. The zero velocity curves in case I for $\mu_1 = 0.502, \mu_2 = 3.579$ and $\mu_1 = 0.991, \mu_2 = 0.704$ are given in Figure 5. The Hill spheres are the circular regions surrounding the four primaries masses shown in Figure 5. It is clear from equation (14) that $C + \Omega \geq 0$. Therefore, $\Omega = -C$ will define a boundary between the region of permitted and prohibited motions. The region of possible motion of m_5 in case I for $\mu_1 = 0.502, \mu_2 = 3.579$ and $\mu_1 = 0.991, \mu_2 = 0.704$ is shown in Figure 6for six different values of Jacobian constant C. The shaded regions represent the permitted regions of motion for the infinitesimal mass m_5. It is numerically confirmed that the permitted regions of motion are connected when $C \geq -4.15$. For decreasing values of C, the permitted regions of motion begin to disconnect. They completely disconnect at $C = -5.52$. It can be seen from Figure 6 that the disconnection occurs in six stages, and hence, the infinitesimal mass m_5 will be completely trapped in the shaded region when $C \leq -5.52$. Similar restrictions exist for all combinations of μ_1 and μ_2. However, the disconnection doesn't always occur in six stages. For small values of μ_2, the disconnection occurs in three stages. For example, when $\mu_1 = 0.965281$ and $\mu_2 = 0.0880651$, the complete disconnection is achieved in three stages at $C = -3.85, C = -3.87$, and $C = -3.95$, and when $\mu_1 = 1.38$ and $\mu_2 = 0.025$, the complete disconnection is achieved in two stages at $C = -3.853$ and $C = -3.865$.

The zero velocity curves in case II for $\mu = 1.73878$ and $\mu = 1$ are given in Figure 7. The Hill spheres are the circular regions surrounding the four primaries' masses as shown in Figure 7. In this case of four equal masses, the regions of permitted motion are connected when $C = -4.4$, partially connected when $C = -4.9$ and completely disconnected when $C = -5$. The regions of motion are given in Figure 8, and when $\mu = 1.73878$, the complete disconnection is achieved in four stages as shown in Figure 9. We have shown the graph of zero-velocity curves and effective potential for case III for $\mu = 3$ and $\mu = 0.01$ in Figure 10, respectively. Similar to case I and case II, the complete disconnection of permitted regions is achieved in multiple stages as presented in two Figures 11 and 12. In the first instance, when $\mu = 0.01$, the complete disconnection is achieved in three stages while for the higher mass ratio of $\mu = 3$, it is achieved in four stages.

4. Equilibrium Solutions

Equilibrium solutions of the restricted problem are the solutions of $\Omega_\zeta(\zeta,\eta) = 0$ and $\Omega_\eta(\zeta,\eta) = 0$. For RK5BP, $\Omega(\zeta,\eta)$ is given in equation (13). The two first derivatives of $\Omega(\zeta,\eta)$ are given as follows:

$$\begin{aligned} \Omega_\zeta(\zeta,\eta) &= \zeta - \frac{(\zeta-1)m}{\left((\alpha+\eta)^2+(\zeta-1)^2\right)^{3/2}} - \frac{(\zeta+1)m}{\left((\alpha+\eta)^2+(\zeta+1)^2\right)^{3/2}} - \frac{\zeta m_2}{\left((\eta-\beta)^2+\zeta^2\right)^{(3/2)}} - \frac{\zeta m_4}{\left(\zeta^2+\eta^2\right)^{(3/2)}}, \\ \Omega_\eta(\zeta,\eta) &= \eta - \frac{m(\alpha+\eta)}{\left((\alpha+\eta)^2+(\zeta-1)^2\right)^{3/2}} - \frac{m(\alpha+\eta)}{\left((\alpha+\eta)^2+(\zeta+1)^2\right)^{3/2}} - \frac{m_2(\eta-\beta)}{\left((\eta-\beta)^2+\zeta^2\right)^{(3/2)}} - \frac{\eta m_4}{\left(\zeta^2+\eta^2\right)^{(3/2)}}. \end{aligned} \tag{15}$$

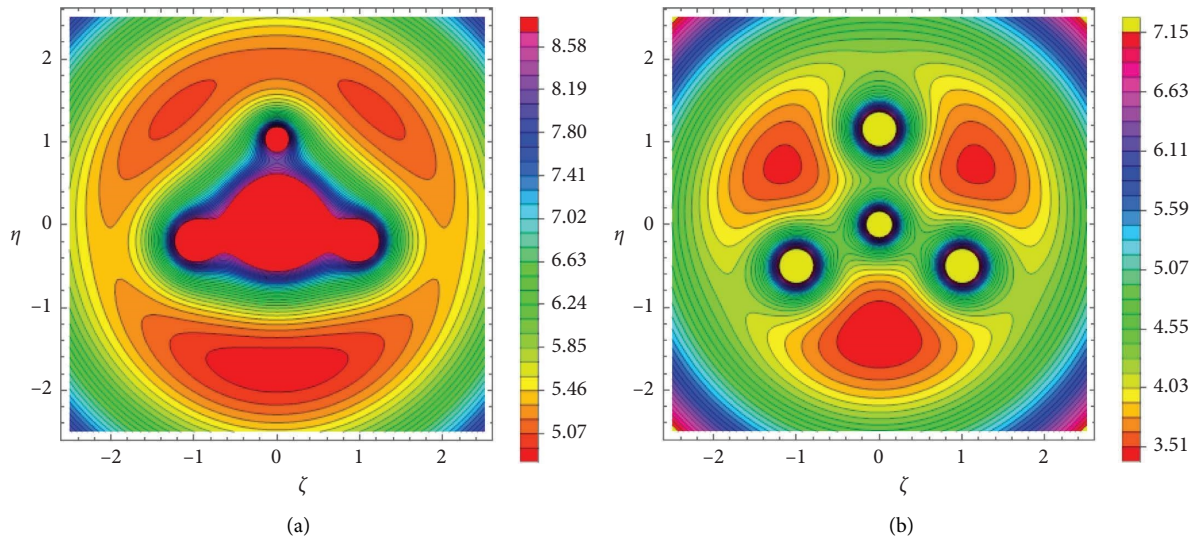

Figure 5: Case I: the evolution of zero velocity curves. (a) $\mu_1 = 0.502, \mu_2 = 3.579$, (b) $\mu_1 = 0.991, \mu_2 = 0.704$.

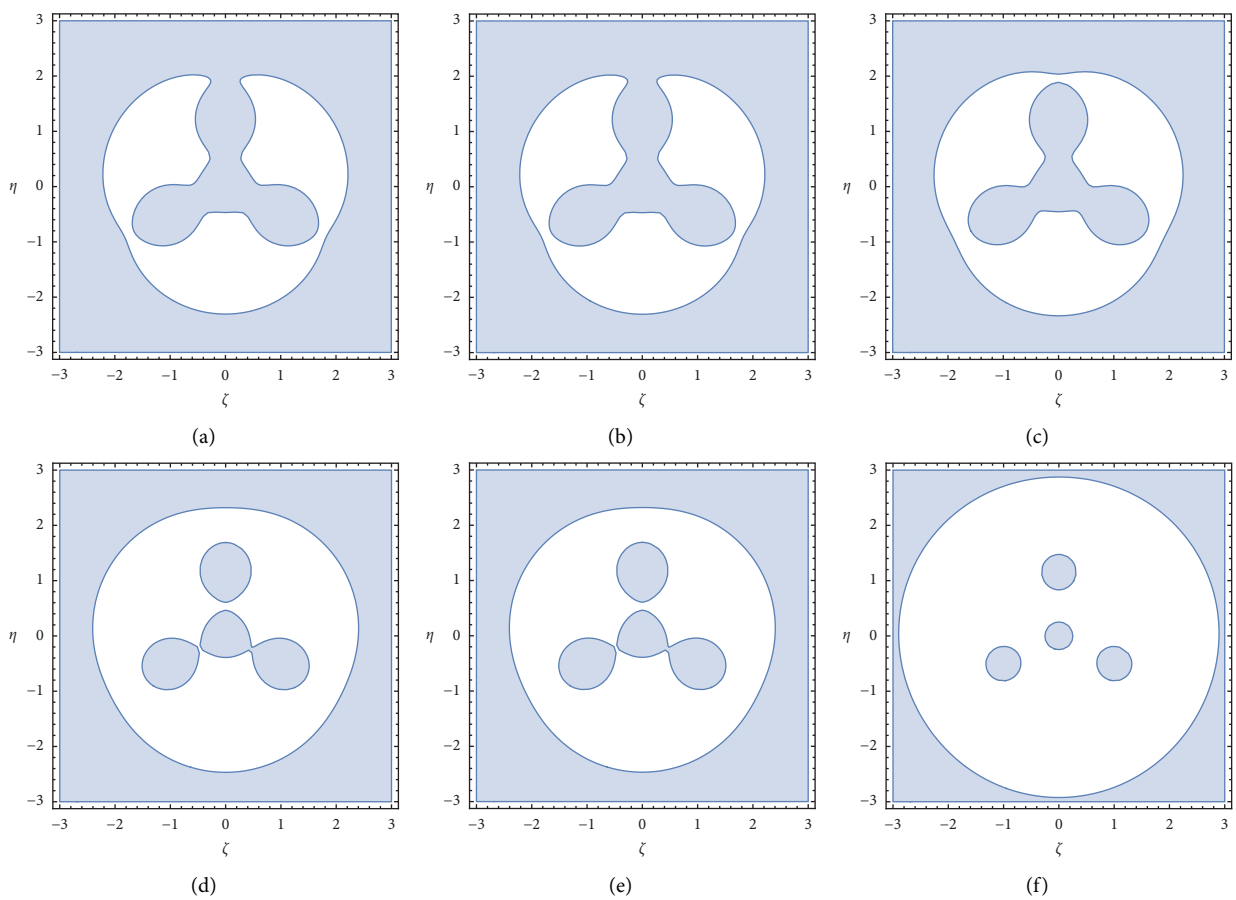

Figure 6: Case I: regions of motion for m_5 when $\mu_1 = 0.99, \mu_2 = 0.704$, (a) $C = -4.15$, (b) $C = -4.22$, (c) $C = -4.27$, (d) $C = -4.5$, (e) $C = -4.51$, (f) $C = -5.52$.

In the following sections, we will study the equilibrium solutions of all three cases introduced in Section 2. Initially, we study the existence and number of equilibrium solutions on the axes and then off the coordinate axes.

4.1. Equilibrium Solutions on the Coordinates Axes

4.1.1. Case I: $m_1 = m_3$. This case is investigated by Gao et al. [23] for equilibrium solutions and zero velocity curves. Our main focus for this case will be on the existence and

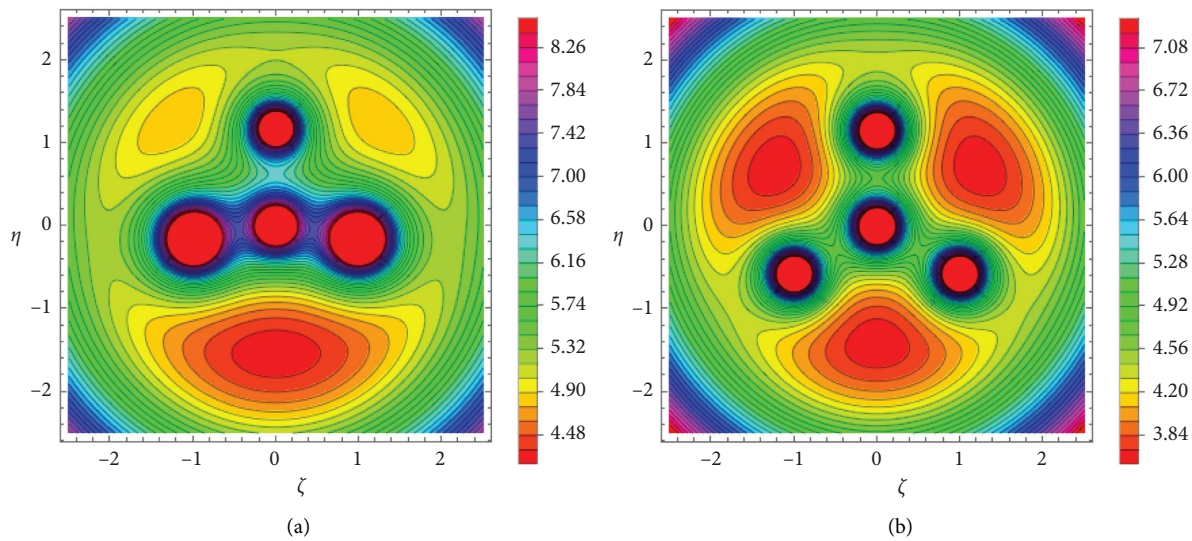

Figure 7: Case II: the evolution of zero velocity curves. (a) $\mu = 1.73878$, (b) $\mu = 1$.

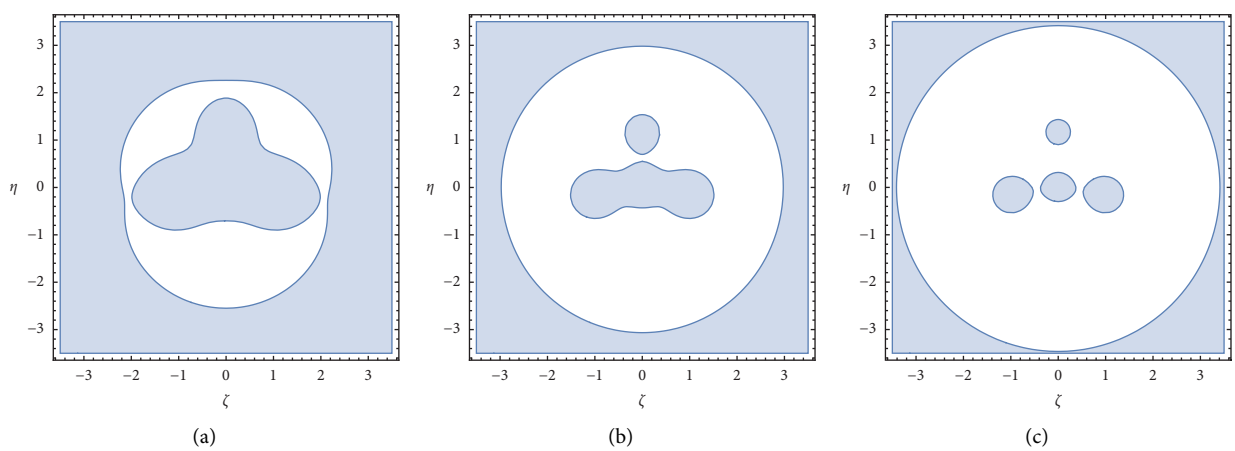

Figure 8: Case II: regions of motion for m_5 when $\mu = 1$ (a) $C = -4.4$, (b) $C = -4.9$, (c) $C = -5$.

uniqueness of equilibrium points. Consider $\zeta = 0$ in $\Omega_\eta(\zeta, \eta) = 0$ and $\Omega_\zeta(\zeta, \eta) = 0$ to investigate the equilibrium solution on the η−axis. These solutions will be obtained from $\Phi_1(\eta) = 0$:

$$\Phi_1(\eta) = -\frac{2(\alpha+\eta)}{\left((\alpha+\eta)^2+1\right)^{(3/2)}} + \frac{\mu_1(\beta-\eta)}{\left((\beta-\eta)^2\right)^{(3/2)}} - \frac{\eta\mu_2}{\left(\eta^2\right)^{(3/2)}} + \eta. \tag{16}$$

We divide η to subintervals $\eta < 0, \eta \in (0, \beta)$ and $\eta > \beta$. The restriction $\eta < 0$ and $\eta > \beta$ will give the solutions which are outside the kite, and $\eta \in (0, \beta)$ will give equilibrium solutions which are inside the concave kite. Consider $\eta \in (0, \beta)$, then $\Phi_1(\eta)$ can be simplified as

$$\Phi_{1a}(\eta) = -\frac{2(\alpha+\eta)}{\left((\alpha+\eta)^2+1\right)^{(3/2)}} + \frac{\mu_1}{(\beta-\eta)^2} - \frac{\mu_2}{\eta^2} + \eta. \tag{17}$$

At $\eta \longrightarrow 0^+$, $\Phi_{1a}(\eta) \longrightarrow -\infty$, and at $\eta \longrightarrow \beta^-$, $\Phi_{1a}(\eta) \longrightarrow +\infty$, and furthermore, $\Phi_{1a}(\eta)$ is continuous on $(0, \beta)$, and therefore, by the mean value theorem, there is at least one zero of $\Phi_{1a}(\eta)$ when $\eta \in (0, \beta)$ and $(\alpha, \beta) \in R_{\mu_1\mu_2}$. The derivative of $\Phi_{1a}(\eta)$ is given by

$$(\Phi_{1a})_\eta(\eta) = -\frac{2}{\left((\alpha+\eta)^2+1\right)^{(3/2)}} + \frac{6(\alpha+\eta)^2}{\left((\alpha+\eta)^2+1\right)^{(5/2)}} + \frac{2\mu_1}{(\beta-\eta)^3} + \frac{2\mu_2}{\eta^3} + 1. \tag{18}$$

Lemma 1. *$(\Phi_{1a})_\eta(\eta)$ positive for $(\alpha, \beta) \in R_{\mu_1\mu_2}$ and $\eta \in (0, \beta)$.*

Proof. The only negative term of $(\Phi_{1a})_\eta(\eta)$ has an absolute maximum value of 2. Consider the first two terms of $(\Phi_{1a})_\eta(\eta)$ and simplifying, we get $4(\alpha+\eta)^2 - 2/((\alpha+\eta)^2+1)^{5/2}$. Solving $= 4(\alpha+\eta)^2 - 2/((\alpha+\eta)^2+1)^{5/2} > 0$ for α and η, one can easily see that $\alpha > 1/\sqrt{2}$ and $\eta > 0$ or $\eta > 1/\sqrt{2}$ and $\alpha > 0$. Now, we need to show that

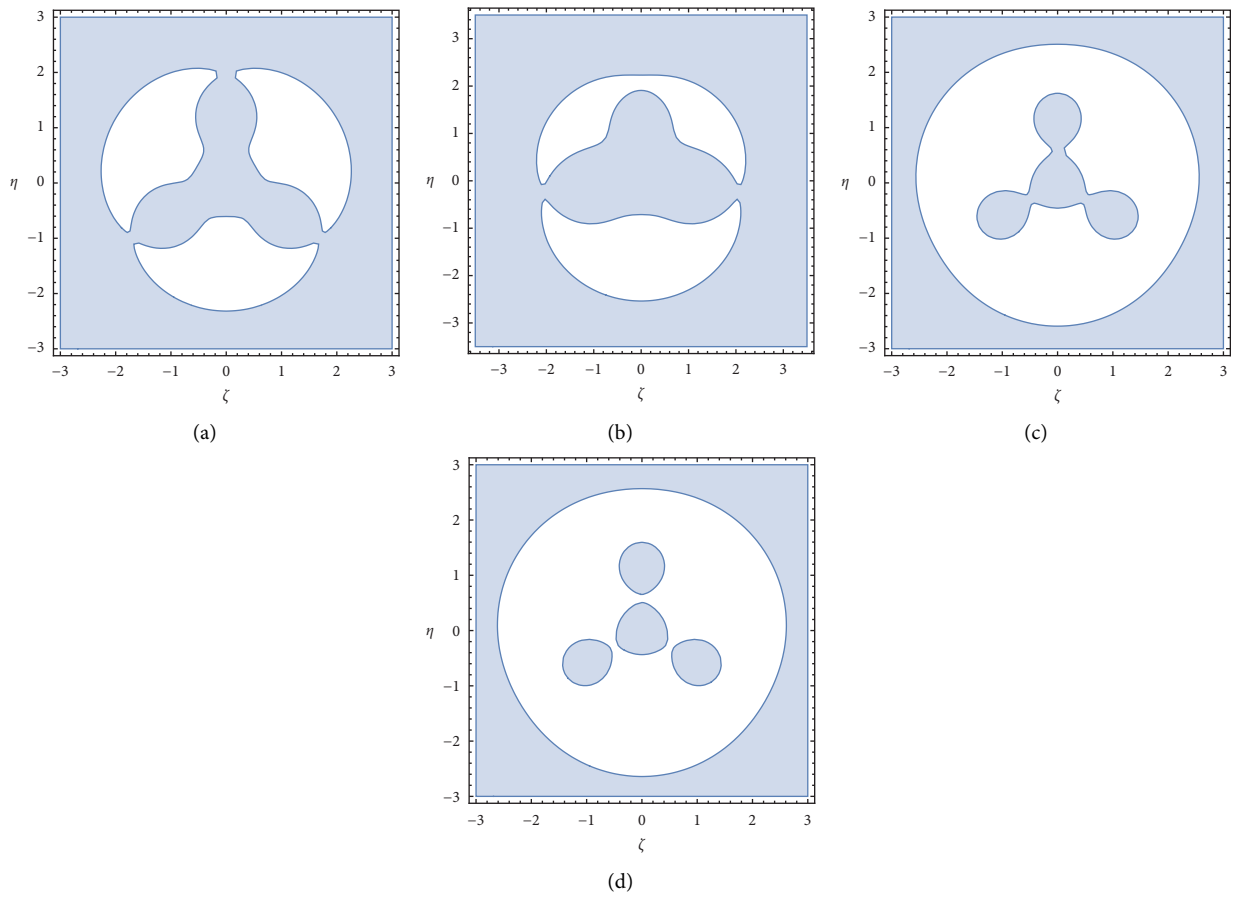

Figure 9: Case II: regions of motion for m_5 when $\mu = 1.73878$ (a) $C = -5.23$, (b) $C = -5.25$, (c) $C = -6.39$, (d) $C = -7.505$.

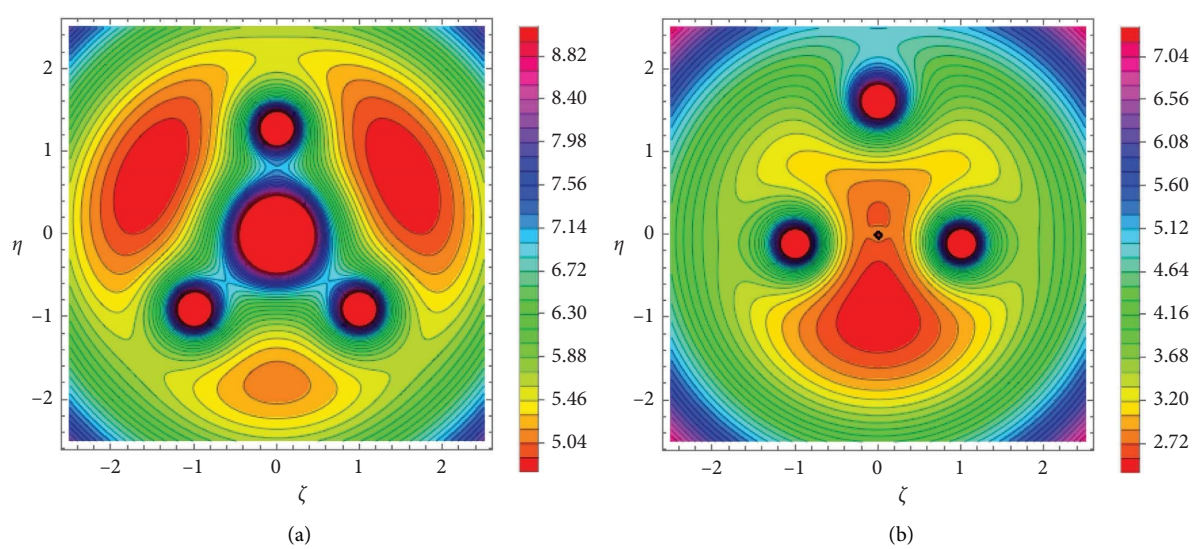

Figure 10: Case III: the evolution of zero velocity curves. (a) $\mu = 3$, (b) $\mu = 0.01$.

$(\Phi_{1a})_\eta(\eta) > 0$ when $\alpha \in (0, 1/\sqrt{2})$ and $\eta \in (0, 1/\sqrt{2})$ since the absolute maximum value of the negative term is -2. We will need to show that the positive terms have a combined minimum value greater than 2. Consider the term $2\mu_2/\eta^3$. The minimum positive value of μ_2 is 0.22, and the maximum value of η is $1/\sqrt{2}$, and therefore, the minimum value

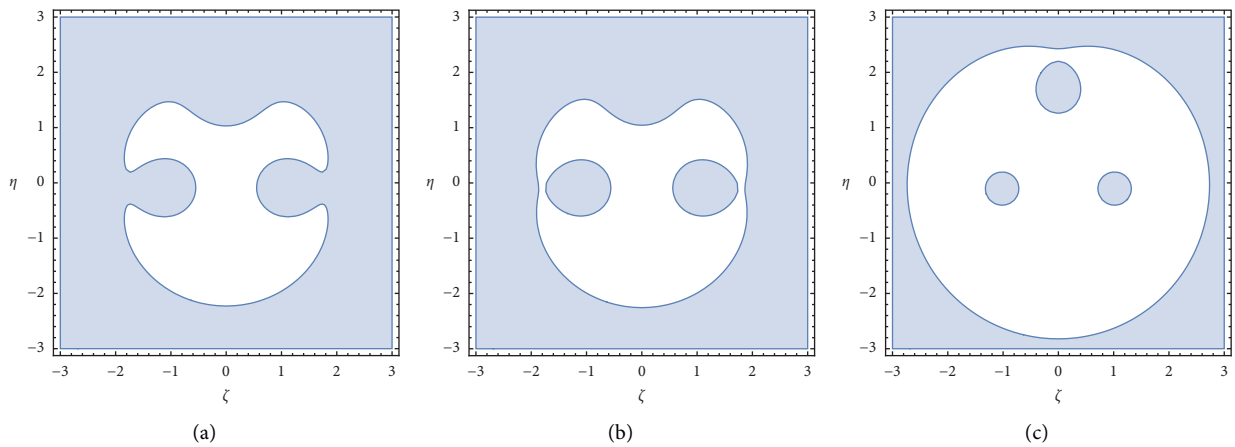

Figure 11: Case III: regions of motion for m_5 when $\mu = 0.01$ (a) $C = -3.6$, (b) $C = -3.65$, (c) $C = -4.9$.

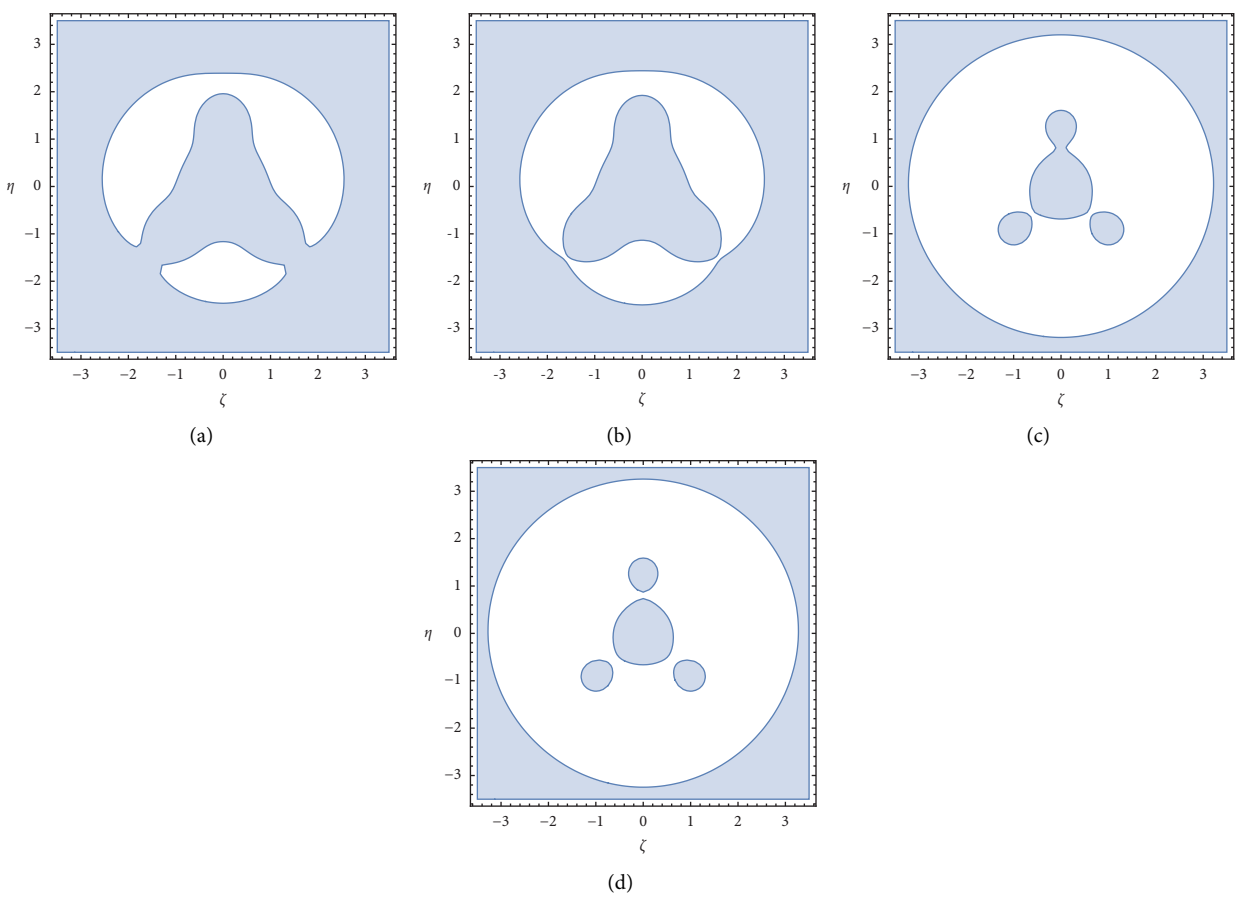

Figure 12: Case III: regions of motion for m_5 when $\mu = 3$ (a) $C = -5.6$, (b) $C = -5.65$, (c) $C = -7.05$, (d) $C = -7.2$.

of η is $1/\sqrt{2}$ as 1.24451. It is now clear that the minimum value of the positive terms of $(\Phi_{1a})_\eta(\eta)$ is greater than 2. This confirms our claim that $(\Phi_{1a})_\eta(\eta) > 0$.

This proves the existence of unique equilibrium solutions inside the concave kite on the η–axis.

Now consider $\eta > \beta$ and rewrite $\Phi_1(\eta)$ as

$$\Phi_{1b}(\eta) = -\frac{2(\alpha+\eta)}{\left((\alpha+\eta)^2+1\right)^{3/2}} - \frac{\mu_1}{(\beta-\eta)^2} - \frac{\mu_2}{\eta^2} + \eta. \quad (19)$$

When $\eta \longrightarrow \beta^+$, the term $-\mu_1/(\beta-\eta)^2$ will increase indefinitely and will dominate the remaining terms therefore

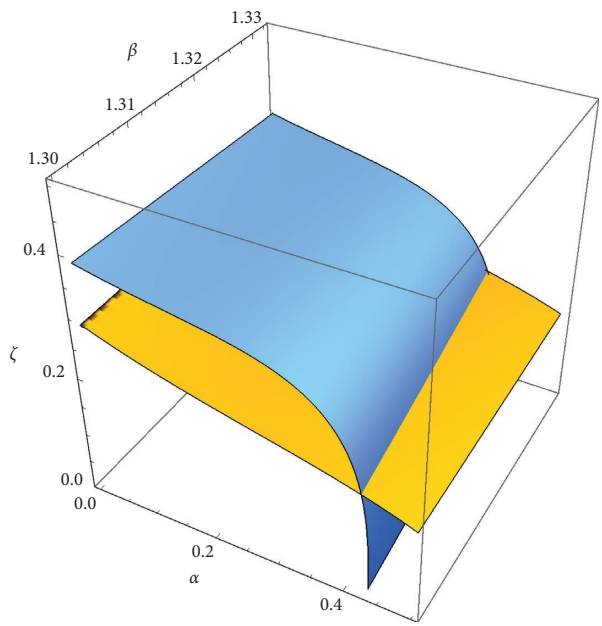

Figure 13: $\Phi_{2a}(\alpha,\beta,\zeta)=0$ and $\Phi_{2b}(\alpha,\beta,\zeta)=0$.

$\Phi_{1b}(\eta)<0$ when $\eta\longrightarrow\beta$. Similarly for large values of $\eta>\beta$, $\alpha\in(0,1)$, and $\beta\in(1,\sqrt{3})$, it is, therefore, trivial to see that η will dominate the negative terms of $\Phi_{1b}(\eta)$ and will change the sign from negative to positive. This proves the existence of equilibrium solutions which are outside the concave kite.

Now, consider the case $\eta<0$ and $\Phi_1(\eta)$ as

$$\Phi_{1c}(\eta)=-\frac{2(\alpha+\eta)}{\left((\alpha+\eta)^2+1\right)^{3/2}}+\frac{\mu_1}{(\beta-\eta)^2}+\frac{\mu_2}{\eta^2}+\eta. \tag{20}$$

It is immediately clear that when $\eta<-\alpha$, $\Phi_{1c}(\eta)>0$, and hence, there are no equilibrium solutions. It can be proved in a way similar to the case of $\eta>\beta$ that there exists a unique equilibrium solution for each $\eta\in(-\alpha,0)$ when $(\alpha,\beta)\in R_{\mu_1\mu_2}$. Therefore, we have a minimum of three solutions on the η–axis two of which will be inside the kite and one outside the kite. For example, when $\alpha=0.5$ and $\beta=1.123$, there are three equilibrium solutions, and when $\alpha=0.5$ and $\beta=1.23$, there are five equilibrium solutions on the η–axis.

Now consider $\eta=0$ in $\Omega_\eta(\zeta,\eta)=0$ and $\Omega_\zeta(\zeta,\eta)=0$. The equilibrium solutions on the ζ–axis will be obtained from the simultaneous solution of $\Phi_{2a}(\zeta)=0$ and $\Phi_{2b}(\zeta)=0$ where

$$\begin{aligned}\Phi_{2a}(\zeta)&=-\frac{\zeta-1}{\phi_a}-\frac{\zeta+1}{\phi_b}+\zeta-\frac{\zeta}{\phi_c}\mu_1\\&\quad-\frac{\zeta}{\left(\zeta^2\right)^{3/2}}\mu_2,\\\Phi_{2b}(\zeta)&=-\frac{\alpha}{\phi_a}-\frac{\alpha}{\phi_b}+\frac{\beta}{\phi_c}\mu_1,\end{aligned} \tag{21}$$

where $\phi_a=(\alpha^2+(\zeta-1)^2)^{3/2}$, $\phi_b=(\alpha^2+(\zeta+1)^2)^{3/2}$, and $\phi_c=(\beta^2+\zeta^2)^{3/2}$. Since $\Phi_{2a}(\zeta)=\Phi_{2a}(-\zeta)$ and $\Phi_{2b}(\zeta)=\Phi_{2b}(-\zeta)$, and therefore, if $\zeta=\zeta_0$ is an equilibrium solution, then $\zeta=-\zeta_0$ will also be an equilibrium solution. Rewrite $\Phi_{2b}(\zeta)$ as

$$\begin{aligned}\Phi_{2a}&=\zeta^2\phi_c\left(\phi_a\left(\zeta\left(\phi_b-1\right)-1\right)-\zeta\phi_b+\phi_b\right)\\&\quad-\phi_a\phi_b\left(\zeta^3\mu_1-\mu_2\phi_c\right),\\\Phi_{2b}&=\beta\phi_a\phi_b\mu_1-\alpha\phi_c\left(\phi_a+\phi_b\right).\end{aligned} \tag{22}$$

It is numerically confirmed from Figure 13 that there are two equilibrium solutions on ζ–axis.

4.1.2. Case II: $m_1=m_3$, $m_2=m_4$. Consider $m_1=m_3=\mu$, $m_2=m_4=1$, and $\zeta=0$ in $\Omega_\eta(\zeta,\eta)=0$ and $\Omega_\zeta(\zeta,\eta)=0$ to find equilibrium solutions on the η–axis. The equilibrium solutions on the η–axis will be obtained from

$$\Phi_3(\eta)=\eta+\frac{\beta-\eta}{\left((\beta-\eta)^2\right)^{3/2}}-\frac{\eta}{\left(\eta^2\right)^{3/2}}-\frac{2\mu(\alpha+\eta)}{\left((\alpha+\eta)^2+1\right)^{3/2}}. \tag{23}$$

In the case when $\eta\in(0,\beta)$, the infinitesimal mass will be inside the kite. It will be outside the kite when $\eta>\beta$ or $\eta<0$. Let $\eta\in(0,\beta)$ and rewrite $\Phi_3(\eta)$ in simplified form

$$\Phi_{3a}(\eta)=-\frac{2\mu(\alpha+\eta)}{\left((\alpha+\eta)^2+1\right)^{3/2}}+\frac{1}{(\beta-\eta)^2}-\frac{1}{\eta^2}+\eta. \tag{24}$$

Because of the term $-1/\eta^2$, $\Phi_{3a}(\eta)\longrightarrow-\infty$ when $\eta\longrightarrow0^+$. Similarly because of the term $1/(\beta-\eta)^2$, $\Phi_{3a}(\eta)>0$ when $\eta\longrightarrow\beta^-$. Therefore, by the mean value theorem, there is at least one equilibrium solution inside the concave kite. The derivative of $\Phi_{3a}(\eta)$ is

$$\begin{aligned}(\Phi_{3a})_\eta(\eta)&=1+\frac{6\mu(\alpha+\eta)^2}{\left((\alpha+\eta)^2+1\right)^{5/2}}+\frac{2}{(\beta-\eta)^3}\\&\quad+\frac{2}{\eta^3}-\frac{2\mu}{\left((\alpha+\eta)^2+1\right)^{3/2}}.\end{aligned} \tag{25}$$

Since $\alpha\in(0,1),\beta(\alpha)\in(1.13,1.26)$ and $\eta\in(0,\beta)$, therefore, the positive terms of $(\Phi_{3a})_\eta(\eta)$ dominate the only negative term, which implies that $(\Phi_{3a})_\eta(\eta)>0$. This proves the existence of a unique equilibrium solution inside the concave kite with two pairs of equal masses. Now, consider $\eta>\beta$ and rewrite $\Phi_3(\eta)$ as

$$\Phi_{3b}(\eta)=\eta-\frac{1}{(\beta-\eta)^2}-\frac{1}{\eta^2}-\frac{2\mu(\alpha+\eta)}{\left((\alpha+\eta)^2+1\right)^{3/2}}. \tag{26}$$

The derivative of $\Phi_{3b}(\eta)$ is

$$\begin{aligned}(\Phi_{3b})_\eta(\eta)&=\frac{6\mu(\alpha+\eta)^2}{\left((\alpha+\eta)^2+1\right)^{5/2}}-\frac{2\mu}{\left((\alpha+\eta)^2+1\right)^{3/2}}\\&\quad-\frac{2}{(\beta-\eta)^3}+\frac{2}{\eta^3}+1.\end{aligned} \tag{27}$$

By the same argument as in the case of $\eta\in(0,\beta)$, the existence of a unique equilibrium solution outside the

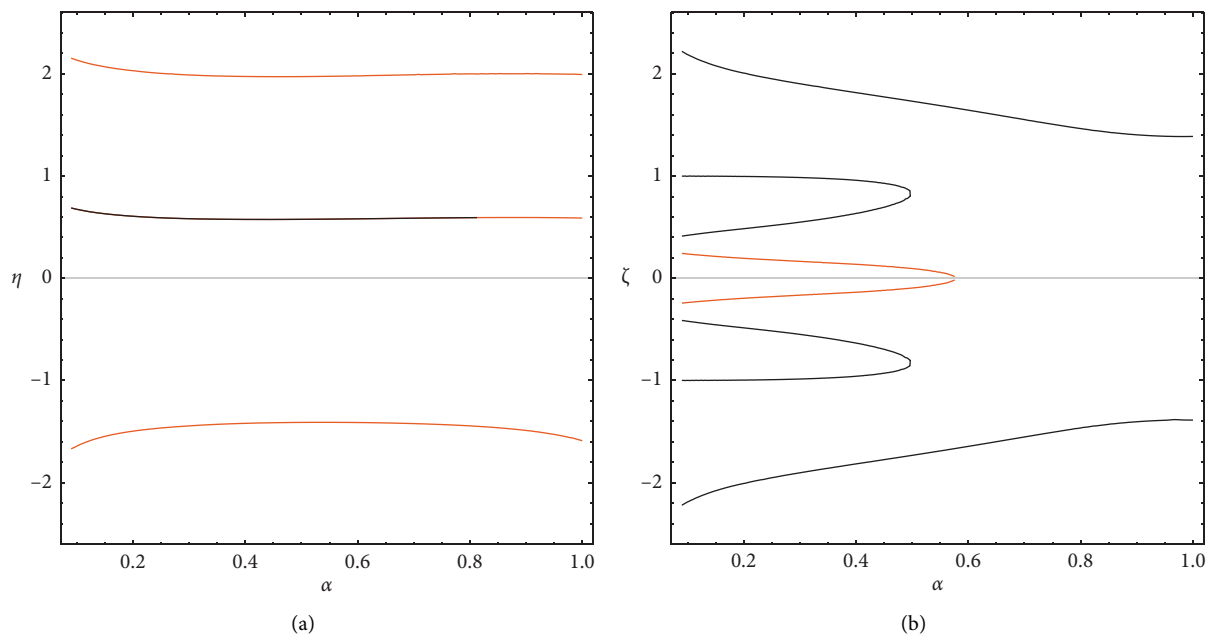

Figure 14: (a) Equilibrium solutions on η−axis when $m_1 = m_3$ and $m_2 = m_4$. The curve shaded black corresponds to the equilibrium solutions which are inside the kite. (b) $\Phi_{4a}(\zeta) = 0$ and $\Phi_{4b}(\zeta) = 0$, and the curve shaded black corresponds to the solutions of $\Phi_{4a}(\zeta) = 0$.

concave kite with two pairs of equal masses is proven. When $\eta < 0$, $\Phi_3(\eta)$ becomes

$$\Phi_{3c}(\eta) = \frac{1}{(\beta-\eta)^2} + \frac{1}{\eta^2} + \eta - \frac{2\mu(\alpha+\eta)}{\left((\alpha+\eta)^2+1\right)^{3/2}}. \tag{28}$$

When $\alpha \in (0,1)$ and $\eta \in (-\alpha, 0)$, the term $1/\eta^2$ dominates the two negative terms η and $2\mu(\alpha+\eta)/((\alpha+\eta)^2+1)^{3/2}$, and hence, $\Phi_{3c}(\eta) > 0$; therefore, there are no equilibrium solutions when $\eta \in (-\alpha, 0)$. Also $\alpha \longrightarrow 0$ implies that $\eta \longrightarrow 0$ implies that $1/\eta^2 \longrightarrow \infty$, and when $\eta \longrightarrow -\alpha$, we get

$$\begin{aligned}\Phi_{3c}(\eta) \longrightarrow \Phi_{3c}(-\alpha) &= \frac{1}{(\beta+\alpha)^2} + \frac{1}{\alpha^2} - \alpha \\ &= \frac{-\alpha^5 - 2\alpha^4\beta - \alpha^3\beta^2 + 2\alpha^2 + 2\alpha\beta + \beta^2}{\alpha^2(\alpha+\beta)^2}.\end{aligned} \tag{29}$$

Since $\beta = \varphi(\alpha) > 0$, by Descartes rule of sign, the polynomial $-\alpha^5 - 2\alpha^4\beta - \alpha^3\beta^2 + 2\alpha^2 + 2\alpha\beta + \beta^2$ has only one real root. It is numerically confirmed that this root is at $\alpha = 1.073$. It is now trivial to show that $\Phi_{3c}(-\alpha) > 0$. When $\eta < -\alpha$, all the terms of $\Phi_{3c}(\eta)$ are positive except η, and therefore, for a sufficiently smaller value of η, $\Phi_{3c}(\eta)$ will become negative. The derivative of $\Phi_{3c}(\eta)$ is

$$\begin{aligned}(\Phi_{3c})_\eta(\eta) = &\frac{6\mu(\alpha+\eta)^2}{\left((\alpha+\eta)^2+1\right)^{5/2}} - \frac{2\mu}{\left((\alpha+\eta)^2+1\right)^{3/2}} \\ &+ \frac{2}{(\beta-\eta)^3} - \frac{2}{\eta^3} + 1.\end{aligned} \tag{30}$$

Since $\eta < -\alpha$, $-2/\eta^3 > 0$, and therefore, only $-2\mu/((\alpha+\eta)^2+1)^{3/2} < 0$ which is clearly dominated by the remaining positive terms, and hence, $(\Phi_{3c})_\eta(\eta) > 0$. This confirms the existence of exactly one equilibrium solution when $\eta < -\alpha$.

Therefore, we have shown that there are three equilibrium solutions on the η−axis. One of the solutions is inside the kite when $\alpha < 0.8$. These solutions are shown in Figure 14.

To find equilibrium points on the ζ− axis, we will need to solve $\Phi_{4a}(\zeta) = 0$ and $\Phi_{4b}(\zeta) = 0$, which are obtained from $\Omega_\zeta(\zeta,\eta) = 0$ and $\Omega_\eta(\zeta,\eta) = 0$, where

$$\begin{aligned}\Phi_{4a}(\zeta) = &-\mu\left(\frac{\zeta-1}{\left(\alpha^2+(\zeta-1)^2\right)^{3/2}} + \frac{\zeta+1}{\left(\alpha^2+(\zeta+1)^2\right)^{3/2}}\right) \\ &- \frac{\zeta}{\left(\beta^2+\zeta^2\right)^{3/2}} \\ &- \frac{\zeta}{\left(\zeta^2\right)^{3/2}} + \zeta, \\ \Phi_{4b}(\zeta) = &\alpha\mu\left(-\frac{1}{\left(\alpha^2+(\zeta+1)^2\right)^{3/2}} - \frac{1}{\left(\alpha^2+(\zeta-1)^2\right)^{3/2}}\right) \\ &+ \frac{\beta}{\left(\beta^2+\zeta^2\right)^{3/2}}.\end{aligned} \tag{31}$$

Since $\Phi_{4a}(\zeta) = -\Phi_{4a}(-\zeta)$ and $\Phi_{4b}(\zeta) = \Phi_{4b}(-\zeta)$, we will therefore only consider $\zeta > 0$. It is numerically confirmed that $\Phi_{4a}(\zeta) = 0$ has one or three zeros on the positive ζ−

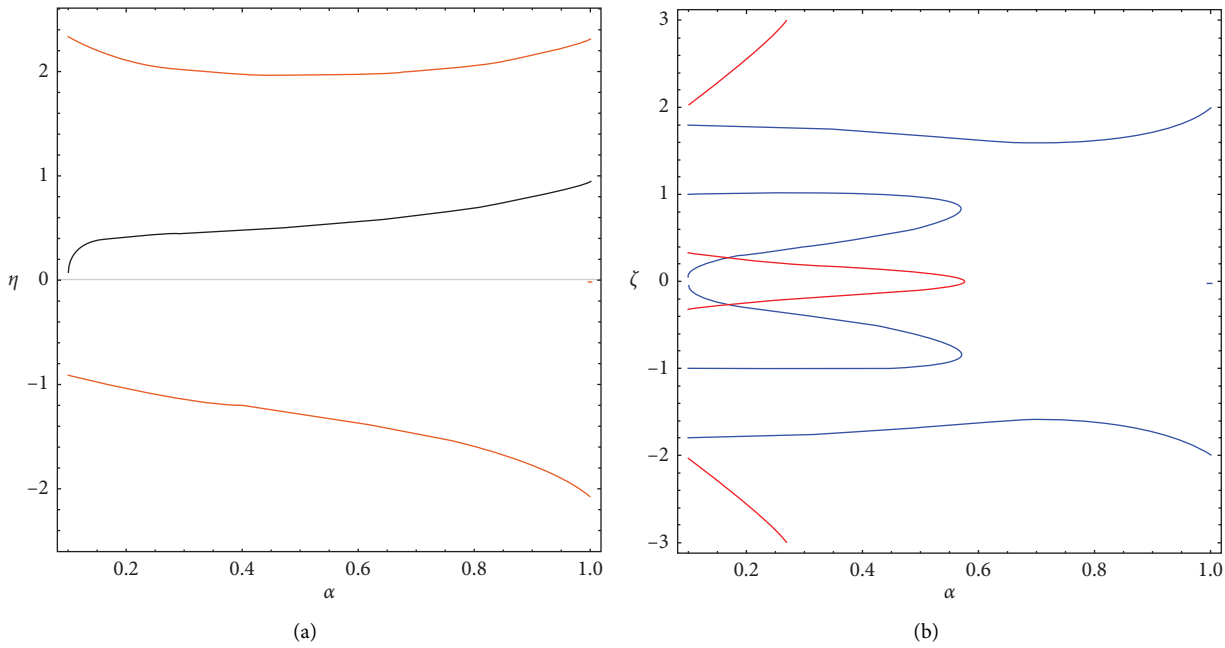

Figure 15: Case III ($m_1 = m_2 = m_3$): (a) equilibrium solutions on η–axis and the red curve corresponds to the solutions of $\Phi_{6b}(\zeta) = 0$, and (b) equilibrium solutions on ζ–axis. The blue curve corresponds to the solutions of $\Phi_{6a}(\zeta) = 0$.

axis. When $\alpha < 0.5$, these solutions occur when $0.4 < \zeta < 2.2$. It is symmetric counterparts are in the interval $-2.2 < \zeta < -0.4$. For $\alpha > 0.5$, there is only one zero when $\zeta > 0$ and another one when $\zeta < 0$. These solutions are shown in Figure 14(b). Similarly, $\Phi_{4b}(\zeta) = 0$ has two zeros when $\zeta \in (-0.25, 0.25)$ and $\alpha < 0.59$. Therefore, there are no equilibrium solutions on the ζ–axis. The curve shaded black corresponds to the solutions of $\Phi_{4a}(\zeta) = 0$.

4.1.3. Case III. Consider $m_1 = m_2 = m_3 = 1$, $\mu = m_4$, and $\zeta = 0$, then equilibria on the η–axis will be the solution of $\Phi_5(\eta) = 0$, where

$$\Phi_5(\eta) = \eta - \frac{2(\alpha+\eta)}{\left((\alpha+\eta)^2+1\right)^{3/2}} + \frac{\beta-\eta}{\left((\beta-\eta)^2\right)^{3/2}} - \frac{\eta}{\left(\eta^2\right)^{3/2}}\mu. \tag{32}$$

The method and procedure to prove the existence and uniqueness of the equilibrium solutions are similar to case I and case II; therefore, we leave the proof of existence and uniqueness to the interested reader and provide only numerical evidence. On the η–axis, there are three equilibrium solutions one of which is inside the Kite. The inside solution is always between m_2 and m_4, and the outside solutions are on either side of m_2 and m_4 outside the triangle formed by m_1, m_2, and m_3. These solutions are shown in Figure 15(a), where the black curve represents the solutions that are inside the kite between m_2 and m_4.

Similarly to get equilibrium solutions on ζ– axis, we substitute $\eta = 0$ in $\Omega_\zeta(\zeta,\eta) = 0$ and $\Omega_\eta(\zeta,\eta) = 0$ which gives $\Phi_{6a}(\zeta) = 0$ and $\Phi_{6b}(\zeta) = 0$, where

$$\begin{aligned}\Phi_{6a}(\zeta) &= \zeta - \frac{\zeta-1}{\left(\alpha^2+(\zeta-1)^2\right)^{3/2}} - \frac{\zeta+1}{\left(\alpha^2+(\zeta+1)^2\right)^{3/2}} \\ &\quad - \frac{\zeta}{\left(\beta(\alpha)^2+\zeta^2\right)^{3/2}} - \frac{\zeta}{\left(\zeta^2\right)^{3/2}}\mu, \\ \Phi_{6b}(\zeta) &= -\frac{\alpha}{\left(\alpha^2+(\zeta-1)^2\right)^{3/2}} - \frac{\alpha}{\left(\alpha^2+(\zeta+1)^2\right)^{3/2}} \\ &\quad + \frac{\beta(\alpha)}{\left(\beta(\alpha)^2+\zeta^2\right)^{3/2}}.\end{aligned} \tag{33}$$

In this case, there are only two equilibrium solutions as shown in Figure 15(b). The solutions are at $(\alpha, \beta, \zeta) = (0.164903, 1.42885, \pm 0.265228)$. In this case, the central mass ($\mu = 0.0907689$) is much smaller than the masses at the vertices of the triangle.

4.2. Equilibrium Solutions Off the Coordinates Axes

4.2.1. Case I. To find a relationship between the masses and the equilibrium points, we define a new mass ratio $\mu_3 = \mu_1/\mu_2$:

$$\mu_3 = \frac{f_3(\alpha,\beta)}{f_4(\alpha,\beta)}, \tag{34}$$

where

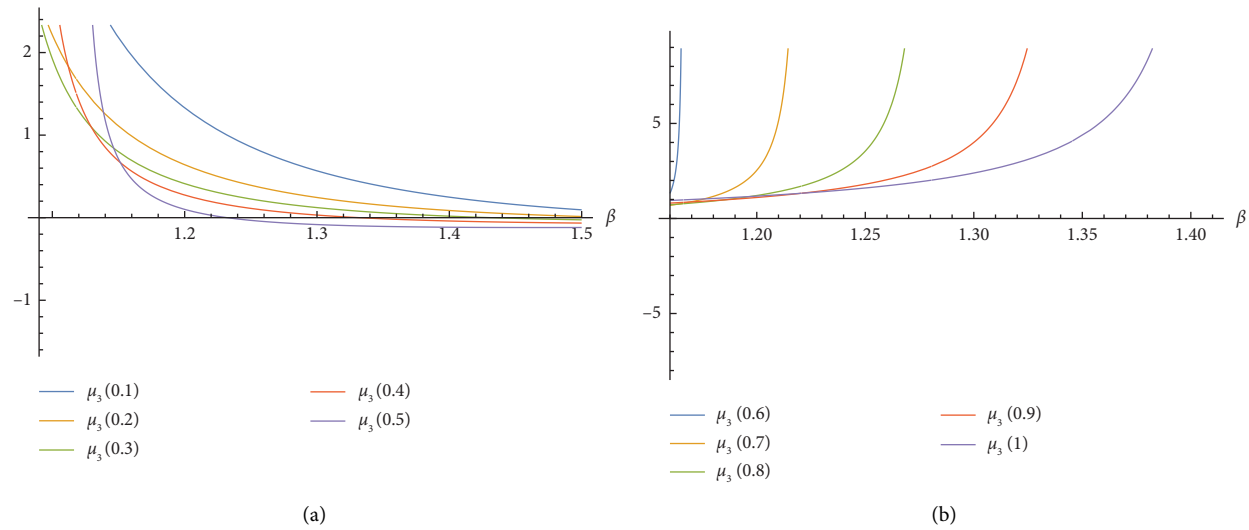

Figure 16: Case I: $\mu_3(\alpha, \beta)$ for fixed values of α.

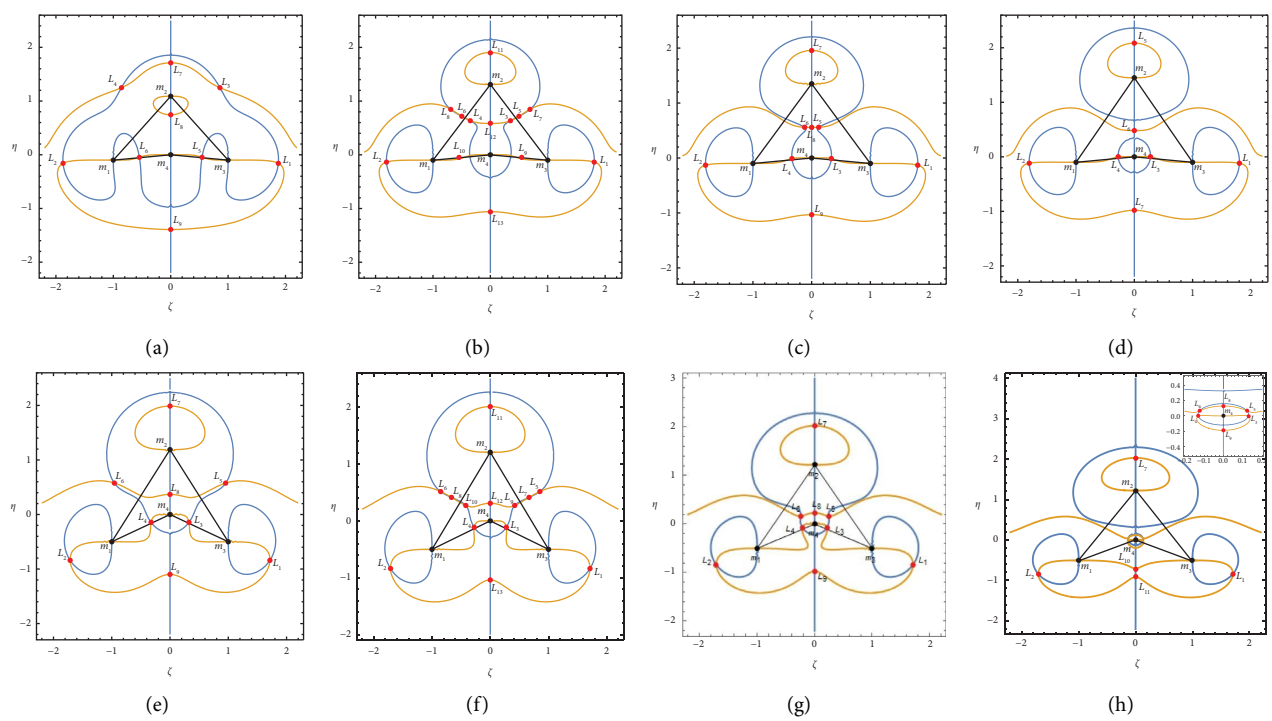

Figure 17: Case I: $\alpha = 0.1$, (a) $\mu_3 = 0.215424$, (b) $\mu_3 = 1.91282$, (c) $\mu_3 = 2.64948$, (d) $\mu_3 = 6.29743$. $\alpha = 0.5$, (e) $\mu_3 = 6.54916$, (f) $\mu_3 = 12.5703$, (g) $\mu_3 = 33.8017$, (h) $\mu_3 = 221.241$.

$$
\begin{aligned}
f_3(\alpha, \beta) &= \left(\alpha^2 + 1\right)^3 (\alpha + \beta)\left(\left(\alpha^2 + 2\alpha\beta + \beta^2 + 1\right)^{3/2} - 8\right) \\
&\quad \cdot \left(\beta^3 - \left((\alpha + \beta)^2 + 1\right)^{3/2}\right), \\
f_4(\alpha, \beta) &= \alpha\left(\left(\alpha^2 + 1\right)^{3/2} - 8\right)\left(\alpha^2 + 2\alpha\beta + \beta^2 + 1\right)^{3/2}\left(\left(\alpha^2 + 1\right)^{3/2} - \beta^3\right) \\
&\quad \cdot \left((\alpha + \beta)^2 + 1\right)^{3/2}.
\end{aligned}
\tag{35}
$$

Table 1: Equilibrium solutions in case I, where L_i represents solutions that are inside the kite, and L_o represents solutions that are outside the kite.

α	μ_3	L_i	L_o
0.1	$\mu_3 < 0.015$	3	4
	[0.015, 1.84)	3	6
	[1.084, 1.995]	5	8
	(1.995, 2.87]	5	4
	$\mu_3 > 2.87$	3	4
0.3	$\mu_3 < 6.45$	3	6
	(6.45, 17.02)	5	8
	[17.02, 79.45)	5	4
	[79.45, 487.5]	3	4
	$\mu_3 > 487.5$	1	4
0.5	$\mu_3 < 10^{-3}$	2	3
	$[10^{-3}, 9.9)$	3	6
	[9.9, 16.09]	5	8
	(16.09, 40.1]	5	4
	(40.1, 335.7]	6	5
	$\mu_3 > 335.7$	2	5
0.6	$\mu_3 > 13.1$	6	3
	[9.5, 13.1]	4	5
	$\mu_3 < 9.5$	3	6
0.8	$\mu_3 > 15.9$	4	3
	[2.1, 15.9]	4	5
	[0.004, 2.1)	3	6
	$\mu_3 < 0.004$	3	4
1	$\mu_3 > 30.5$	4	3
	(3.05, 30.5]	2	5
	(0.87, 3.05]	4	5
	(0.015, 0.87)	3	6
	$\mu_3 \leq 0.015$	3	4

For all the masses to remain positive, we choose α and β from $R_{\mu_1\mu_2}$ given in equation (6). Based on the values of α, the region $R_{\mu_1\mu_2}$ is divided into two parts, i.e., when $0 < \alpha < 1/\sqrt{3}$ and $\alpha > 1/\sqrt{3}$. When $0 < \alpha < 1/\sqrt{3}$, μ_3 is a decreasing function of β for fixed value of α and is an increasing function when $\alpha > 1/\sqrt{3}$ as shown in Figure 16.

Depending on the distance between the central mass m_4 and m_1 or m_3, the number of equilibrium points changes from seven to thirteen. This effect is best explained by Figure 17. When $\alpha = 0.1$, the equilibrium points are distributed as follows which shows a clear dependence on the ratio between m_2 and m_4. The equilibrium solutions in case I are shown in Table 1 for different values of α ranging between 0.1 and 1.

4.2.2. Case II and Case III. In the case when $m_1 = m_3$ and $m_2 = m_4$ (case II), there are a total of 9 equilibrium points. These include the three equilibriums which were shown to exist on the η−axis. The remaining 6 equilibrium points are off the axes. There is no change in the number of equilibrium points for the varying values of any of the masses are parameters. The parameter α or the mass relation μ only affects the position of the equilibrium points. This effect is best explained in Figure 18.

In the case when $m_1 = m_2 = m_3$ and $m_4 = \mu(\alpha)$, the number of equilibrium points depends on α and hence $\mu(\alpha)$. For $\alpha = 0.11$, there are only four equilibrium points as shown in Figure 19(a). Two of the four equilibrium points are on the η−axis. For $\alpha \in (0.11, 0.18)$, there are seven equilibrium points with three inside the kite and four outside the kite, as shown in Figure 19(b). For $\alpha \in [0.18, 0.2$, there are nine equilibrium points with five inside the kite and four outside the kite, shown in Figure 19(c). For $\alpha \in [0.2, 0.23)$, there are eleven equilibrium points with five inside the kite and six outside the kite, shown in Figure 19(d). For $\alpha \in [0.23, 0.26)$, the number of equilibrium points increases to 13 with five inside and 8 outside the kite; however, for $\alpha \geq 0.26$, the number of equilibrium points reduces to nine with three inside the kite and six outside the kite. There is a clear trend of dependence of equilibrium points on α when $\alpha < 0.26$; however, the trend is broken when $\alpha \geq 0.26$, and therefore, we cannot conclude that the number of equilibrium either depends on the parameter α or the masses.

5. Stability Analysis of Equilibrium Points

To study the stability of the equilibrium points, the standard procedure of linearization is followed. Let the location of an equilibrium point in the RK5BP be denoted by (ζ, η) and consider a small displacement (x, y) to the new position $(\zeta + x, \eta + y)$. Using Taylor's series expansion, a new set of second-order linear differential equations is obtained.

$$\begin{aligned} \ddot{x} - 2\dot{y} &= x\Omega_{\zeta\zeta} + y\Omega_{\zeta\eta}, \\ \ddot{y} + 2\dot{x} &= x\Omega_{\zeta\eta} + y\Omega_{\eta\eta}. \end{aligned} \tag{36}$$

The matrix form of the linearized equations is

$$\dot{\mathbf{X}} = \mathscr{A}\mathbf{X}, \tag{37}$$

where

$$\mathbf{X} = \begin{pmatrix} \dot{x} \\ \dot{y} \\ \ddot{x} \\ \ddot{y} \end{pmatrix}, \qquad \mathscr{A} = \begin{pmatrix} 0 & 0 & 1 & 0 \\ 0 & 0 & 0 & 1 \\ \Omega_{\zeta\zeta} & \Omega_{\zeta\eta} & 0 & 2 \\ \Omega_{\zeta\eta} & \Omega_{\eta\eta} & -2 & 0 \end{pmatrix}. \tag{38}$$

For ζ and η to be a stable solution, all the eigenvalues of $\mathscr{A}$ must be pure imaginary. To find these eigenvalues, write the characteristic polynomial for $\mathscr{A}$ as

$$\lambda^4 + F_1\lambda^2 + F_2 = 0, \tag{39}$$

where $F_1 = 4 - \Omega_{\zeta\zeta} - \Omega_{\eta\eta}$ and $F_2 = \Omega_{\zeta\zeta}\Omega_{\eta\eta} - \Omega_{\zeta\eta}^2$. For λ to be pure imaginary, we must either $F_1 > 0$ and $0 < F_2 \leq F_1^2/4$ or $F_1 > 0$ and $F_1^2 = 4F_2$. We will numerically identify regions where at least one of the above conditions is satisfied. In case I, when $m_1 = m_3$, the stability regions for two values of α are given in Figure 20. Upon inspection, it is seen that none of the corresponding equilibrium points are in the stability region, and hence, the equilibrium points are unstable. We

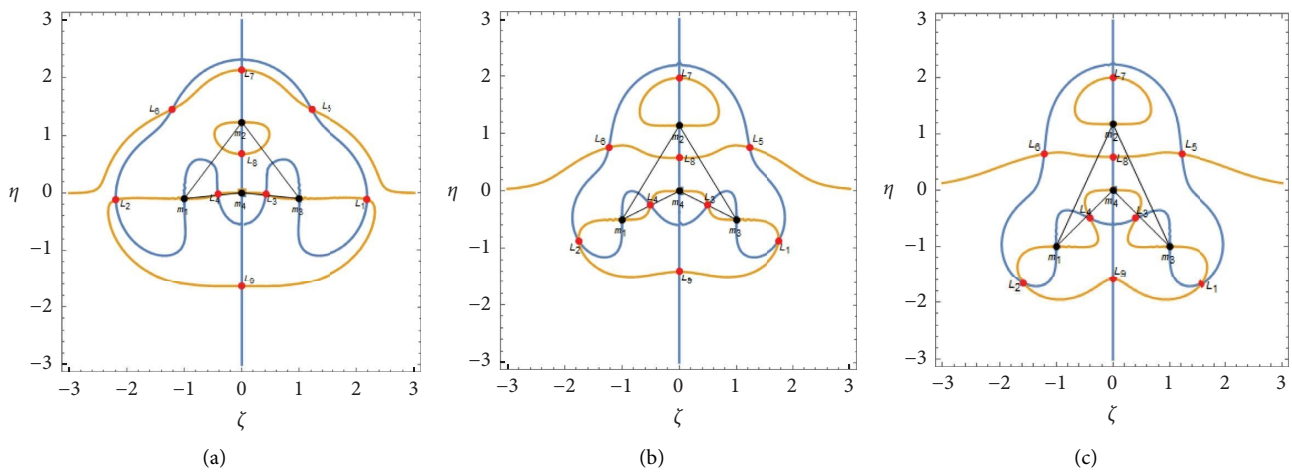

Figure 18: Case II: (a) $\alpha = 0.1$, $\mu = 2.30816$, (b) $\alpha = 0.5$, $\mu = 1.02436$, (c) $\alpha = 1$, $\mu = 1.40976$.

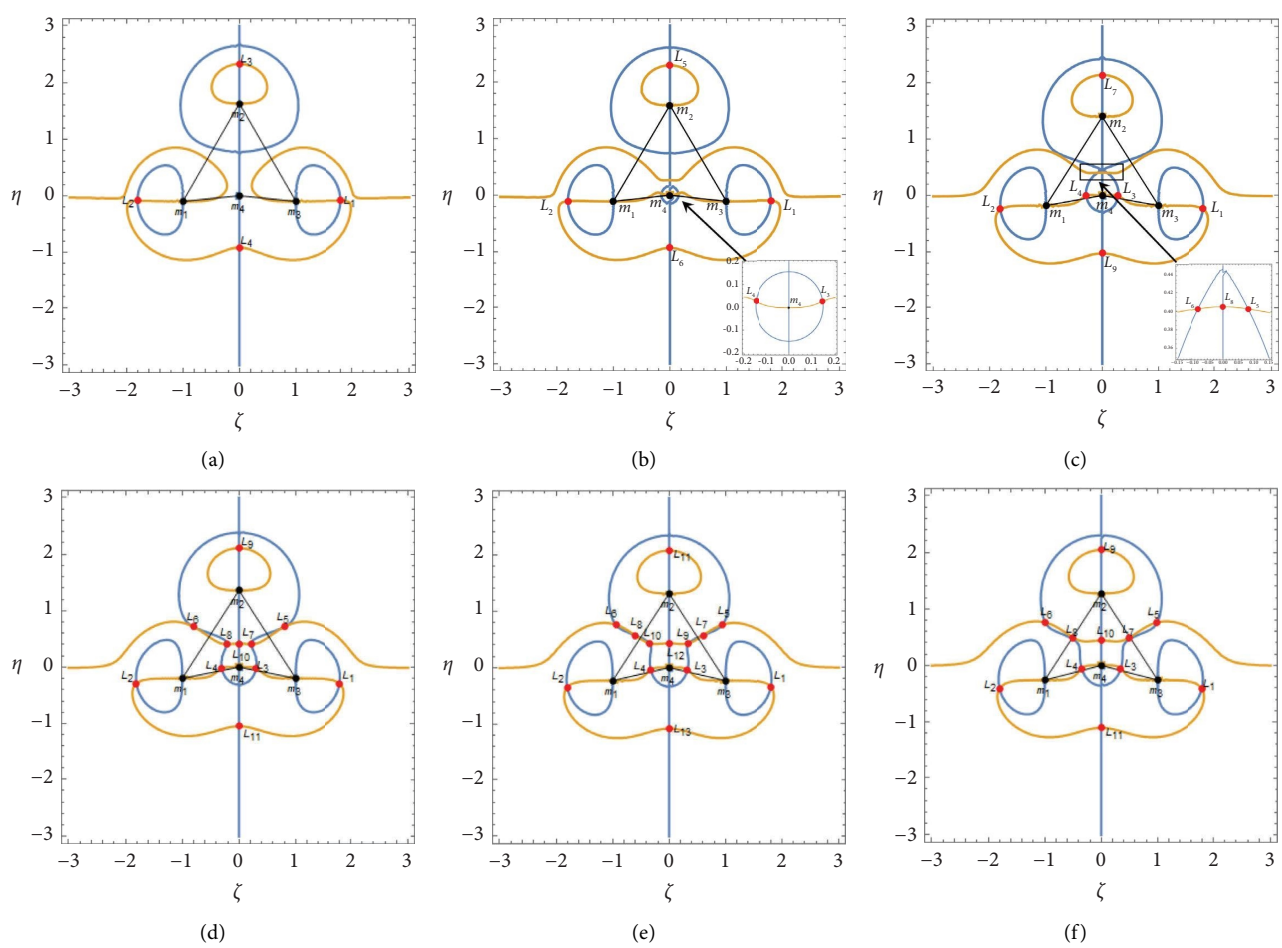

Figure 19: Case III: (a) $\alpha = 0.1$, $\mu = 0.000870568$, (b) $\alpha = 0.11$, $\mu = 0.015408$, (c) $\alpha = 0.18$, $\mu = 0.110342$, (d) $\alpha = 0.2$, $\mu = 0.135761$, (e) $\alpha = 0.23$, $\mu = 0.17328$, (f) $\alpha = 0.26$, $\mu = 0.210775$.

have taken many values of α and tested the equilibrium points for stability; however, none of the equilibrium points are stable. Some representative examples are given in Tables 2 to 4. Similarly, stability regions for case II and case III are given in Figure 21, and however, it has been numerically confirmed that none of the equilibrium points intersects the stability regions, and hence, all the equilibrium points are unstable. Examples are given in Tables 2 to 4.

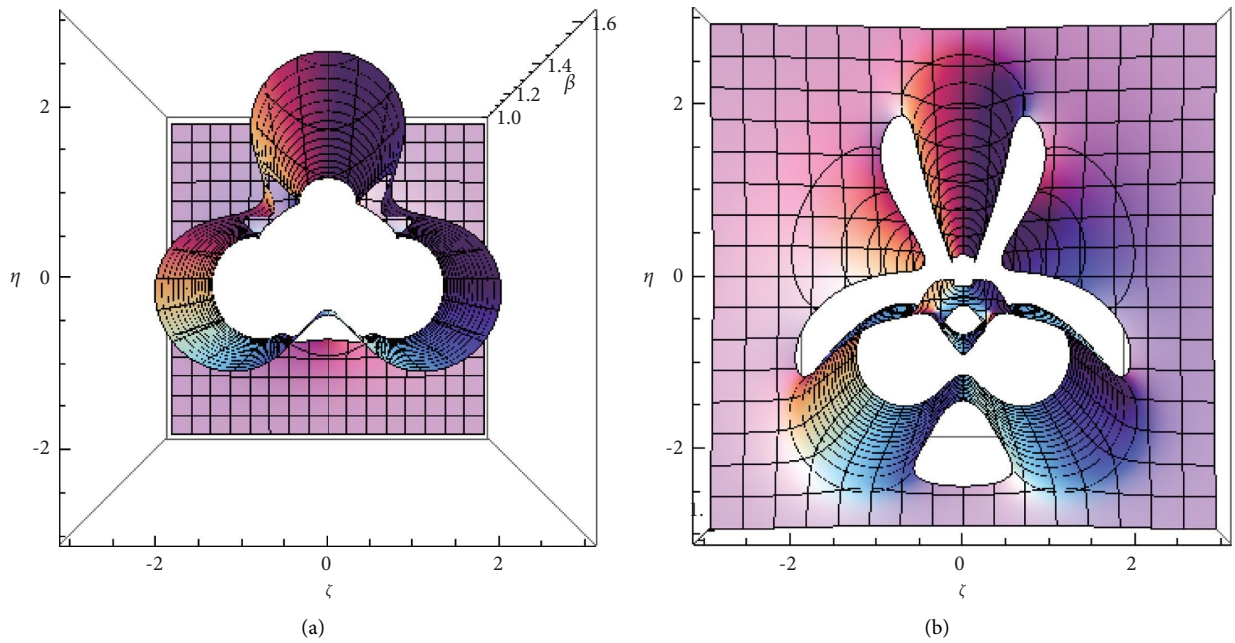

Figure 20: Case I: stability regions when (a) $\alpha = 0.1$ and (b) $\alpha = 1.5$.

Table 2: Equilibrium points and stability analysis for case I.

α	β	Equilibrium points	Eigenvalues
1.67735	1.9	$(0, -3.408225)$	$\pm 0.061374 \pm 0.625297i$
1.67735	0.5	$(1.287412, -2.246649)$	$\pm 2.45214, \pm 2.0193i$
1.0	0.75	$(-0.290910, 0.156697)$	$\pm 0.700942 \pm 0.795715i$
1.0	1.3	$(-0.556749, 0.598284)$	$\pm 3.94186, \pm 2.92914i$
0.1	1.09	$(0, -1.391427)$	$\pm 0.561054 \pm 0.897934i$
0.1	1.09	$(0.545500, -0.048450)$	$\pm 6.11196, \pm 4.43349i$

Table 3: Equilibrium points and stability analysis for case II.

α	β	Equilibrium points	Eigenvalues
0.7	1.175	$(-0.491563, -0.35767)$	$\pm 4.03479, \pm 2.98474i$
0.7	1.175	$(-1.209520, 0.640767)$	$\pm 0.790083 \pm 0.990442i$
0.6	1.157	$(0, 0.581854)$	$\pm 4.39023, \pm 3.23182i$
0.6	1.157	$(0, 0.411430)$	$\pm 0.81095 \pm 0.991591i$
0.001	1.651	$(0.144835, 0.000365)$	$\pm 31.8258, \pm 22.5228i$
0.001	1.651	$(0, 5.342432)$	$\pm 0.111266 \pm 0.713724i$

Table 4: Equilibrium points and stability analysis for case III.

α	β	Equilibrium points	Eigenvalues
0.99	1.355	$(-1.748638, 0.781904)$	$\pm 1.87133, \pm 1.51809i$
0.99	1.355	$(0, 0.926791)$	$\pm 5.89049, \pm 3.93221i$
0.1	1.630	$(0, 0.075206)$	$\pm 1.46199 \pm 0.990952i$
0.1	1.630	$(0.045407, 0.035441)$	$\pm 0.07061, \pm 2.14825i$

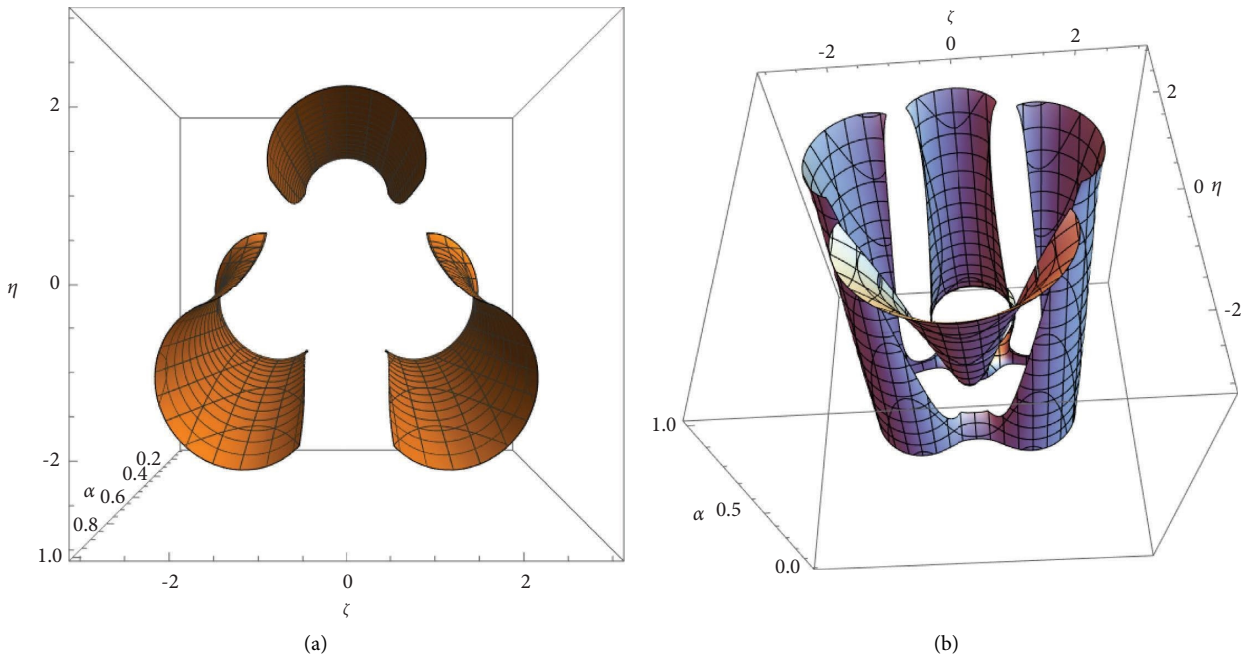

Figure 21: Stability regions (a) case II and (b) case III.

6. Conclusion

In this paper, we studied the motion of a body of negligible mass under the Newtonian gravitational attraction of four bodies (primaries). The primaries move in circular periodic orbits around their center of mass and maintain their geometric arrangement at all times. We have considered here three cases of central configuration based on the masses of the four primaries placed at the vertices of a concave kite. Using analytical techniques, regions of central configurations are derived for all three cases. To complement the analytical results, these regions are also explored numerically. The fifth mass (negligible mass with respect to the primaries) is moving in the gravitational field of four primaries. We have obtained equations of motion of the infinitesimal mass moving in the plane of motion of the primaries in synodical coordinates to get rid of the time dependency of the equation of motion of m_5. The equations of motion of m_5 are nonlinear ordinary differential equations. We did a qualitative analysis of the equation of motion of m_5 and found equilibrium solutions for the infinitesimal mass for all three different cases of the central configuration of the four primaries. We investigated the uniqueness and existence of equilibrium points on the coordinate axes and numerically off the coordinate axes. We can confirm that the number of equilibrium points is between 7 and 13 for three cases of central configuration for different values of mass parameters. The linear stability analysis revealed that none of the equilibrium points are stable. Additionally, we have obtained the permissible region of motions for m_5 in the field of four primaries in kite configuration according to the Jacobian constant. The Hill sphere and the zero velocity curves of primaries are also discussed.

Data Availability

No data were used to support this study.

Conflicts of Interest

The authors declare that they have no conflicts of interest.

References

[1] D. G. Saari, "Central configurations—a problem for the twenty-first century," *Exped. Math. MAA Spectrum*, pp. 283–295, 2011.

[2] R. Moeckel, "Central configurations," *Scholarpedia*, vol. 9, no. 4, Article ID 10667, 2014.

[3] S. Farantos, *Nonlinear Hamiltonian Mechanics Applied to Molecular Dynamics*, Springer, New York, NY, USA, 2014.

[4] C. Deng and S. Zhang, "Planar symmetric concave central configurations in Newtonian four-body problems," *Journal of Geometry and Physics*, vol. 83, pp. 43–52, 2014.

[5] W. D. MacMillan and W. Bartky, "Permanent configurations in the problem of four bodies," *Transactions of the American Mathematical Society*, vol. 34, no. 4, pp. 838–875, 1932.

[6] C. Sim, "Relative equilibrium solutions in the four body problem," *Celestial Mechanics*, vol. 18, no. 2, pp. 165–184, 1978.

[7] J. Llibre and L. F. Mello, "New central configurations for the planar 5-body problem," *Celestial Mechanics and Dynamical Astronomy*, vol. 100, no. 2, pp. 141–149, 2008.

[8] K. E. Papadakis and S. S. Kanavos, "Numerical exploration of the photogravitational restricted five-body problem," *Astrophysics and Space Science*, vol. 310, no. 1-2, pp. 119–130, 2007.

[9] M. Kulesza, M. Marchesin, and C. Vidal, "Restricted rhomboidal five-body problem," *Journal of Physics A: Mathematical and Theoretical*, vol. 44, no. 48, Article ID 485204, 2011.

[10] M. A. R. Siddique, A. R. Kashif, M. Shoaib, and S. Hussain, "Stability analysis of the rhomboidal restricted six-body problem," *Advances in Astronomy*, vol. 2021, Article ID 5575826, 15 pages, 2021.

[11] A. A. Ansari and Z. A. Alhussain, "The restricted five-body problem with cyclic kite configuration," *Journal of Dynamical Systems and Geometric Theories*, vol. 17, no. 1, pp. 91–107, 2019.

[12] M. Shahbaz Ullah, K. B. Bhatnagar, and M. R. Hassan, "Sitnikov problem in the cyclic kite configuration," *Astrophysics and Space Science*, vol. 354, no. 2, pp. 301–309, 2014.

[13] A. Bengochea, A. Hernández-Garduño, and E. Pérez-Chavela, "New families of periodic orbits in the 4-body problem emanating from a kite configuration," *Applied Mathematics and Computation*, vol. 398, Article ID 125961, 2021.

[14] M. Hampton, "Finiteness of kite relative equilibria in the five-vortex and five-body problems," *Qualitative Theory of Dynamical Systems*, vol. 8, no. 2, pp. 349–356, 2009.

[15] M. Álvarez-Ramírez and J. Llibre, "Hjelmslev quadrilateral central configurations," *Physics Letters A*, vol. 383, no. 2-3, pp. 103–109, 2019.

[16] B. Érdi and Z. Czirják, "Central configurations of four bodies with an axis of symmetry," *Celestial Mechanics and Dynamical Astronomy*, vol. 125, no. 1, pp. 33–70, 2016.

[17] B. Benhammouda, A. Mansur, M. Shoaib, I. Szücs-Csillik, and D. Offin, "Central configurations and action minimizing orbits in kite four-body problem," *Advances in Astronomy*, vol. 2020, Article ID 5263750, 18 pages, 2020.

[18] M. Hampton, "Stacked central configurations: new examples in the planar five-body problem," *Nonlinearity*, vol. 18, no. 5, pp. 2299–2304, 2005.

[19] L. F. Mello and A. C. Fernandes, "Co-circular and co-spherical kite central configurations," *Qualitative theory of dynamical systems*, vol. 10, no. 1, pp. 29–41, 2011.

[20] E. Perez-Chavela and M. Santoprete, "Convex four-body central configurations with some equal masses," *Archive for Rational Mechanics and Analysis*, vol. 185, no. 3, pp. 481–494, 2007.

[21] M. Corbera, J. M. Cors, and G. E. Roberts, "A four-body convex central configuration with perpendicular diagonals is necessarily a kite," *Qualitative theory of dynamical systems*, vol. 17, no. 2, pp. 367–374, 2018.

[22] A. A. Ansari, A. Ali, M. Alam, and R. Kellil, "Cyclic kite configuration with variable mass of the fifth body in r5bp," *Applications and Applied Mathematics: International Journal*, vol. 14, no. 2, p. 23, 2019.

[23] C. Gao, J. Yuan, and C. Sun, "Equilibrium points and zero velocity surfaces in the axisymmetric restricted five-body problem," *Astrophysics and Space Science*, vol. 362, no. 4, p. 72, 2017.